

**REPORT ON A HELICOPTER-BORNE
VERSATILE TIME DOMAIN ELECTROMAGNETIC (VTEM max) AND
AEROMAGNETIC GEOPHYSICAL SURVEY**

Mamadawerre Project

Northwest, East 1 and East 2 Blocks

Northern Territory, Australia

For:

Alligator Energy Limited

By:

Geotech Ltd.

245 Industrial Parkway North

Aurora, ON, CANADA, L4G 4C4

Tel: 1.905.841.5004

Fax: 1.905.841.0611

www.geotech.ca

Email: info@geotech.ca

Survey flown during November 2014

Project AA140346

January, 2015

TABLE OF CONTENTS

EXECUTIVE SUMMARY	iii
1. INTRODUCTION	1
1.1 General Considerations	1
1.2 Survey and System Specifications	2
1.3 Topographic Relief and Cultural Features	3
2. DATA ACQUISITION	6
2.1 Survey Area	6
2.2 Survey Operations	6
2.3 Flight Specifications	7
2.4 Aircraft and Equipment	7
2.4.1 Survey Aircraft	7
2.4.2 Electromagnetic System	7
2.4.3 Airborne magnetometer	11
2.4.4 FULL WAVEFORM VTEM Sensor Calibration	11
2.4.5 Radar Altimeter	11
2.4.6 GPS Navigation System	11
2.4.7 Digital Acquisition System	11
2.5 Base Station	12
3. PERSONNEL	13
4. DATA PROCESSING AND PRESENTATION	14
4.1 Flight Path	14
4.2 Electromagnetic Data	14
4.3 Magnetic Data	15
5. DELIVERABLES	16
5.1 Survey Report	16
5.2 Maps	16
5.3 Digital Data	16
6. CONCLUSIONS AND RECOMMENDATIONS	21

LIST OF FIGURES

Figure 1: Property Location	1
Figure 2: Survey areas location on Google Earth	2
Figure 3: Flight path over a Google Earth Image - Northwest	3
Figure 4: Flight path over a Google Earth Image – East 1	4
Figure 5: Flight path over a Google Earth Image – East 2	5
Figure 6: VTEM Transmitter Current Waveform	7
Figure 7: VTEM max System Configuration	10
Figure 8: Z, X and Fraser filtered X (FFx) components for “thin” target	15

LIST OF TABLES

Table 1: Survey Specifications	6
Table 2: Survey schedule	6
Table 3: Off-Time Decay Sampling Scheme	8
Table 4: Acquisition Sampling Rates	11
Table 5: Geosoft GDB Data Format	17
Table 6: Geosoft Resistivity Depth Image GDB Data Format	19
Table 7: Geosoft database for the VTEM waveform	19

APPENDICES

A. Survey location maps
B. Survey Block Coordinates
C. Geophysical Maps
D. Generalized Modelling Results of the VTEM System.....
E. EM Time Constant (TAU) Analysis
F. TEM Resistivity Depth Imaging (RDI).....
G. Resistivity Depth Images (RDI)

REPORT ON A HELICOPTER-BORNE VERSATILE TIME DOMAIN ELECTROMAGNETIC (VTEM max) and AEROMAGNETIC SURVEY

Mamadawerre Project
Northern Territory, Australia

EXECUTIVE SUMMARY

During November 3rd to 13th, 2014 Geotech Ltd. carried out a helicopter-borne geophysical survey over the Mamadawerre Project blocks Northwest, East 1 and East 2 situated near Jabiru NT, Australia.

Principal geophysical sensors included a versatile time domain electromagnetic (VTEM max) system, and a caesium magnetometer. Ancillary equipment included a GPS navigation system and a radar altimeter. A total of 533 line-kilometres of geophysical data were acquired during the survey.

In-field data quality assurance and preliminary processing were carried out on a daily basis during the acquisition phase. Preliminary and final data processing, including generation of final digital data and map products were undertaken from the office of Geotech Ltd. in Aurora, Ontario.

The processed survey results are presented as the following maps:

- Electromagnetic stacked profiles of the B-field Z Component,
- Electromagnetic stacked profiles of dB/dt Z Components,
- Colour grids of a B-Field Z Component Channel,
- Fraser Filtered dB/dt X Component,
- Total Magnetic Intensity (TMI), and
- EM Time-constant dB/dt Z Component (Tau).

Digital data includes all electromagnetic and magnetic products, plus ancillary data including the waveform.

The survey report describes the procedures for data acquisition, processing, final image presentation and the specifications for the digital data set.

1. INTRODUCTION

1.1 General Considerations

Geotech Ltd. performed a helicopter-borne geophysical survey over the Mamadawerre Project blocks Northwest, East 1 and East 2 situated approximately 90 kilometres northeast of Jabiru, NT (Figure 1 & Figure 2).

Rob Sowerby represented Alligator Energy Limited during the data acquisition and data processing phases of this project.

The geophysical surveys consisted of helicopter borne EM using the versatile time-domain electromagnetic (VTEM max) with full receiver-waveform streamed data recorded system with Z and X component measurements and aeromagnetics using a caesium magnetometer. A total of 533 line-km of geophysical data were acquired during the survey.

The crew was based out of Myra Camp (Figure 2) in Northern Territory for the acquisition phase of the survey. Survey flying started on November 3rd and was completed on November 13th, 2014.

Data quality control and quality assurance, and preliminary data processing were carried out on a daily basis during the acquisition phase of the project. Final data processing followed immediately after the end of the survey. Final reporting, data presentation and archiving, were completed from the Aurora office of Geotech Ltd. in January 2015.

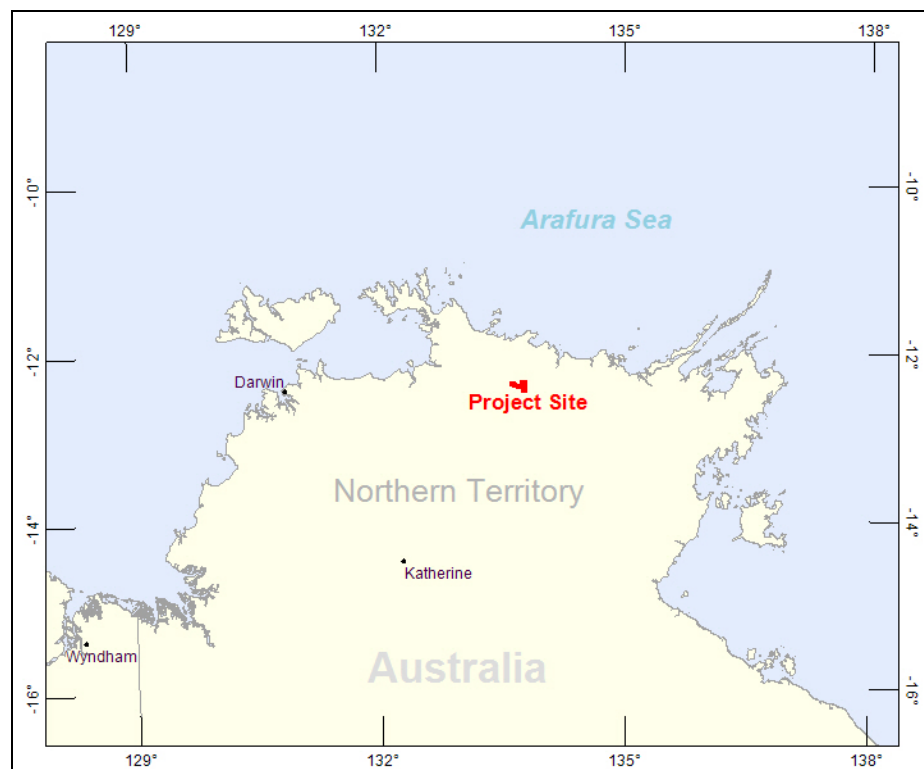


Figure 1: Property Location.

1.2 Survey and System Specifications

The blocks are located approximately 90 kilometres northeast of Jabiru NT, Australia (Figure 2).

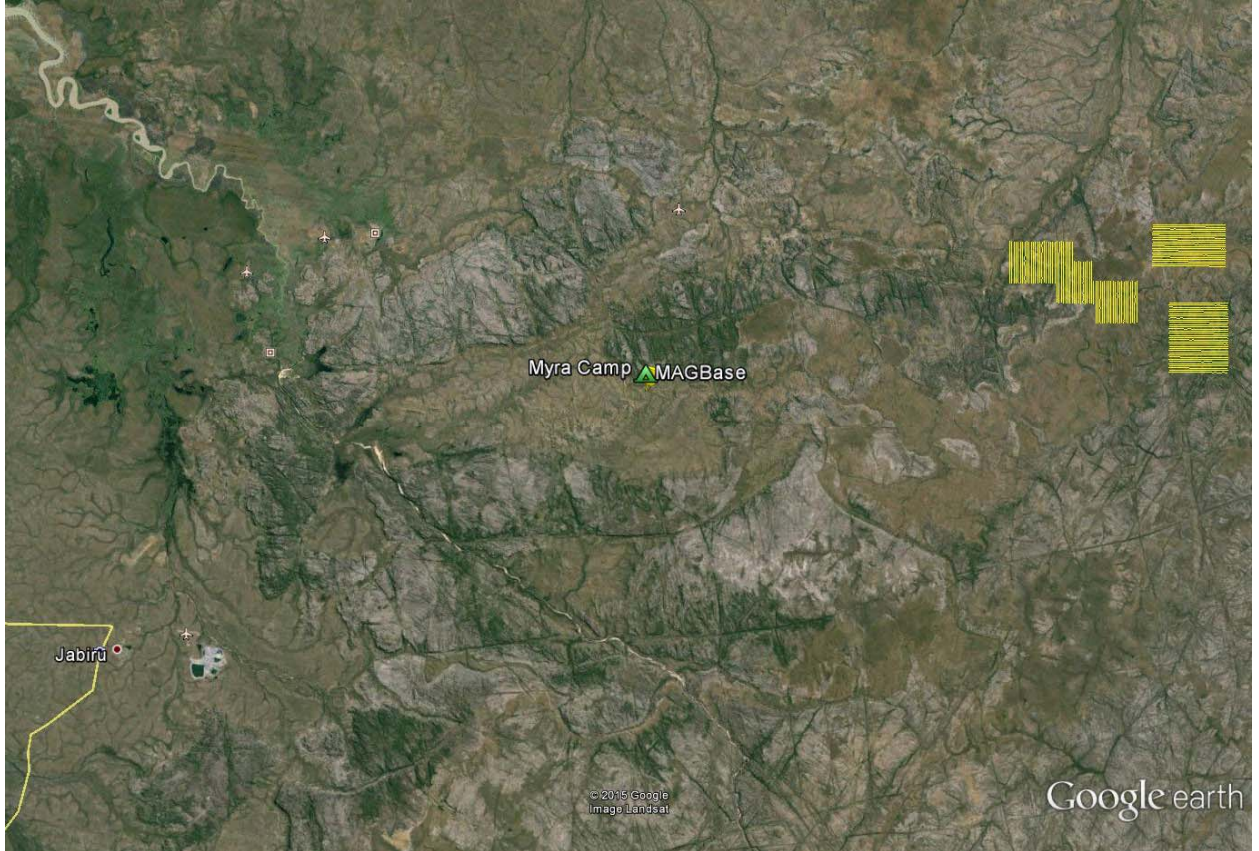


Figure 2: Survey areas location on Google Earth.

The Northwest Block was flown in a south to north (N 0° E azimuth) direction, with traverse line spacing of 200 metres and the East 1 and East 2 Blocks were flown in an east to west (N 90° E azimuth) direction as depicted in Figure 3. Tie lines were neither planned nor flown. For more detailed information on the flight spacing and direction see Table 1.

1.3 Topographic Relief and Cultural Features

Topographically, the block exhibits a shallow relief with an elevation ranging from 30 to 311 metres above mean sea level over an area of 111 square kilometres (Figure 3 - 5).

The blocks have various rivers and streams running through the area, which connect various lakes. There are no visible signs of culture such as roads, trails or buildings throughout the survey area.

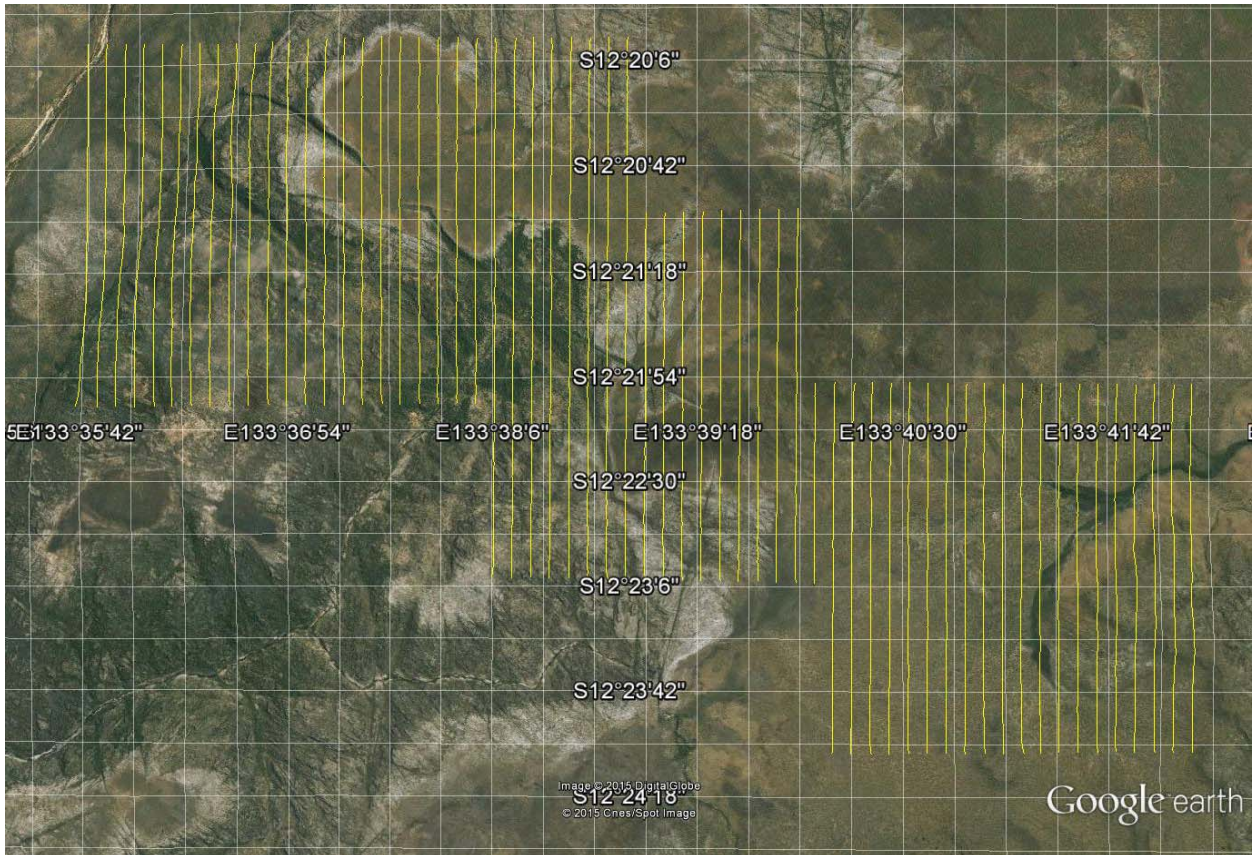


Figure 3: Flight path over a Google Earth Image - Northwest

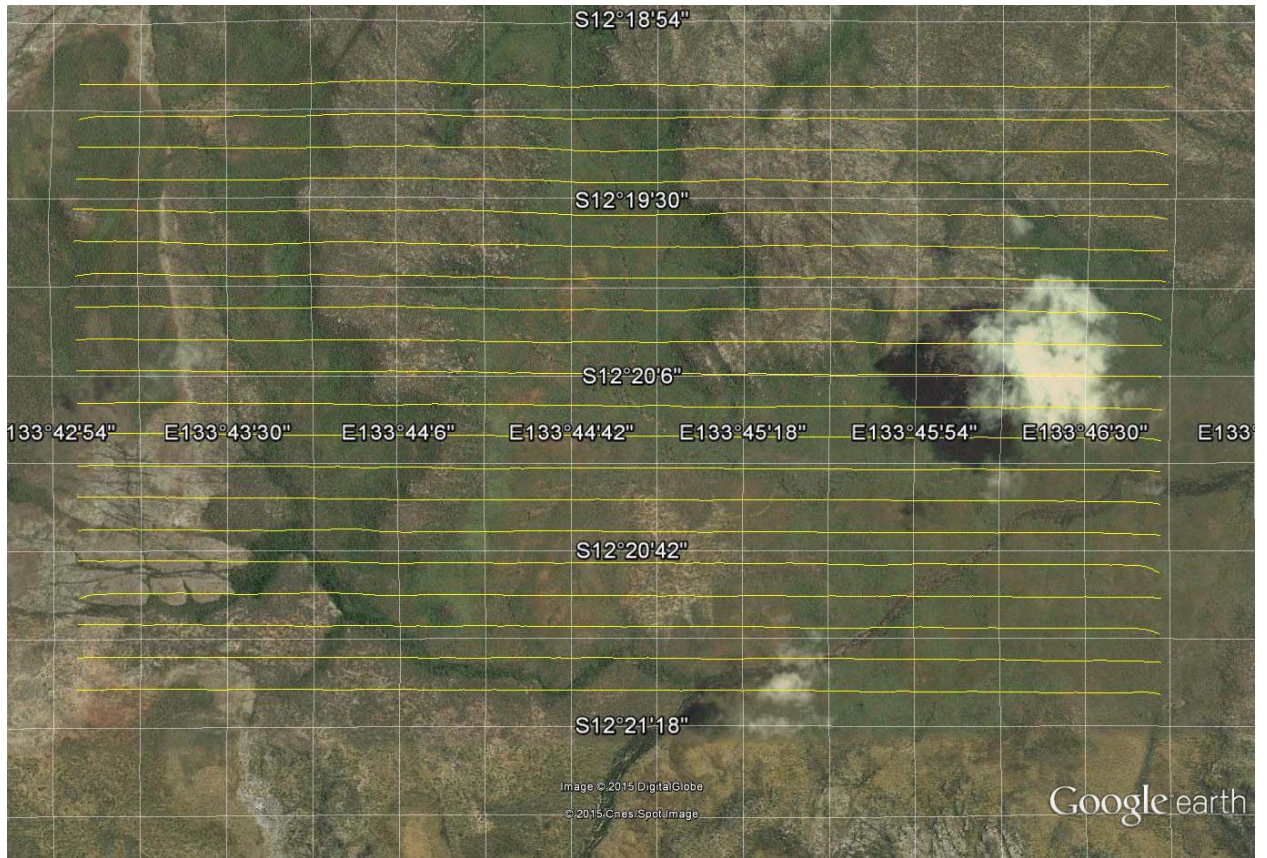


Figure 4: Flight path over a Google Earth Image – East 1

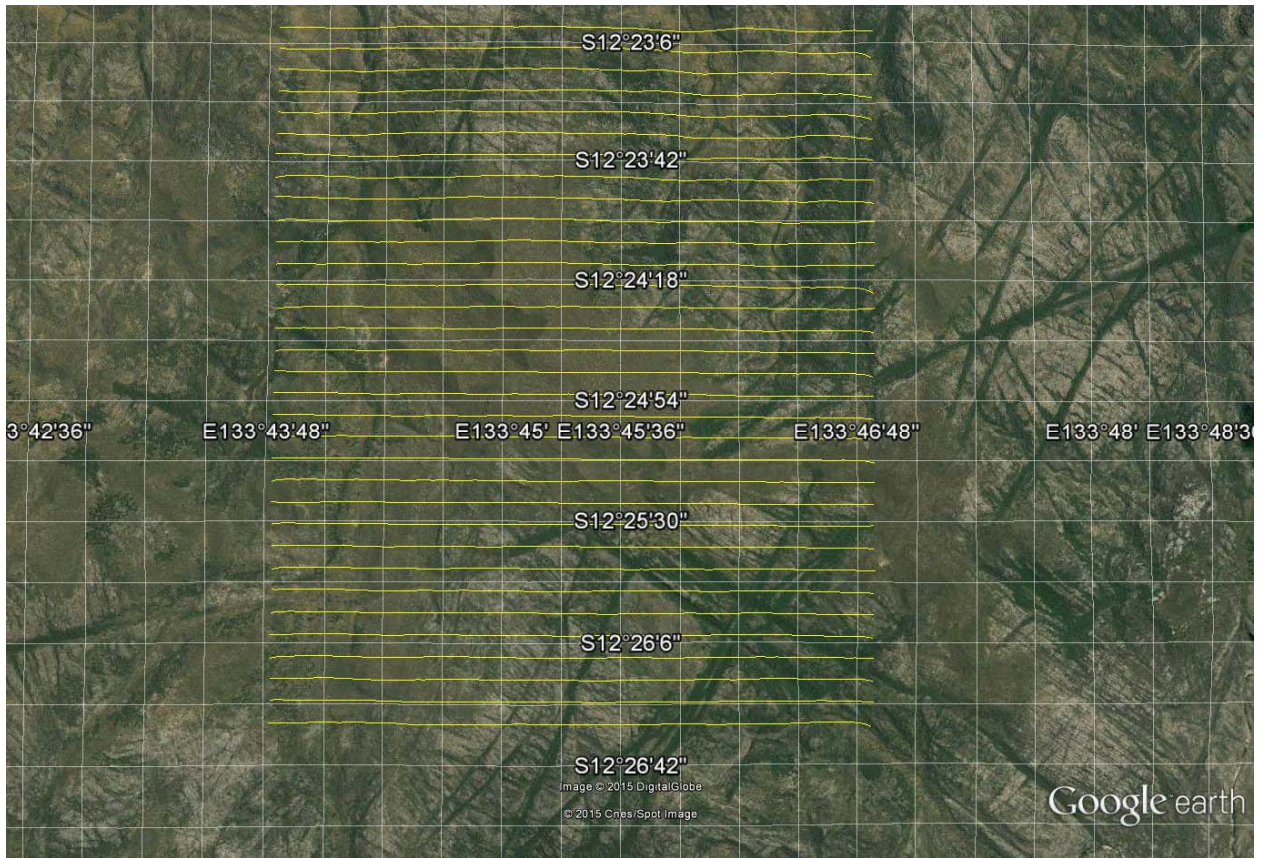


Figure 5: Flight path over a Google Earth Image – East 2

2. DATA ACQUISITION

2.1 Survey Area

The survey block (see Figure 3 and Appendix A) and general flight specifications are as follows:

Table 1: Survey Specifications

Survey block	Line spacing (m)	Area (Km ²)	Planned ¹ Line-km	Actual Line-km	Flight direction	Line numbers
Northwest	Traverse: 200	48	228	245.7	N 0° E / N 180° E	L20010 – L20600
East 1	Traverse: 200	27	132	137.2	N 90° E / N 270° E	L10010 – L10200
East 2	Traverse: 200	36	173	182.5	N 90° E / N 270° E	L10370– L10690
TOTAL		111	533	565.4		

Survey block boundaries co-ordinates are provided in Appendix B.

2.2 Survey Operations

Survey operations were based out of Myra Camp, Northern Territory from November 3rd to November 13th, 2014. The following table shows the timing of the flying.

Table 2: Survey schedule

Date	Flight #	Flown km	Block	Crew location	Comments
3-Nov-2014				Myra Camp, NT Australia	Crew arrived
4-Nov-2014				Myra Camp, NT Australia	System assembly
5-Nov-2014				Myra Camp, NT Australia	System assembly
6-Nov-2014				Myra Camp, NT Australia	System assembly
7-Nov-2014				Myra Camp, NT Australia	Helicopter maintenance
8-Nov-2014				Myra Camp, NT Australia	Helicopter maintenance
9-Nov-2014				Myra Camp, NT Australia	Testing & troubleshooting
10-Nov-2014				Myra Camp, NT Australia	Testing & troubleshooting
11-Nov-2014	1,2	54	NW	Myra Camp, NT Australia	54km flown
12-Nov-2014	3,4,5,6	279	NW	Myra Camp, NT Australia	279km flown
13-Nov-2014	7,8,9	205	E1&2	Myra Camp, NT Australia	Remaining kms were flown – flying complete

¹ Note: Actual Line kilometres represent the total line kilometres in the final database. These line-km normally exceed the Planned line-km, as indicated in the survey NAV files.

2.3 Flight Specifications

During the survey the helicopter was maintained at a mean altitude of 85 metres above the ground with an average survey speed of 80 km/hour. This allowed for an actual average EM transmitter-receiver loop terrain clearance of 42 metres and a magnetic sensor clearance of 75 metres.

The on board operator was responsible for monitoring the system integrity. He also maintained a detailed flight log during the survey, tracking the times of the flight as well as any unusual geophysical or topographic features.

On return of the aircrew to the base camp the survey data was transferred from a compact flash card (PCMCIA) to the data processing computer. The data were then uploaded via ftp to the Geotech office in Aurora for daily quality assurance and quality control by qualified personnel.

2.4 Aircraft and Equipment

2.4.1 Survey Aircraft

The survey was flown using an Agusta AW119 Koala helicopter, registration VH-VTQ. The helicopter is owned and operated by United Aero Helicopters. Installation of the geophysical and ancillary equipment was carried out by a Geotech Ltd crew.

2.4.2 Electromagnetic System

The electromagnetic system was a Geotech Time Domain EM (VTEM max) full receiver-waveform streamed data recorded system. The “full waveform VTEM system” uses the streamed half-cycle recording of transmitter and receiver waveforms to obtain a complete system response calibration throughout the entire survey flight. VTEM, with the serial number 24 had been used for the survey. The VTEM transmitter current waveform is shown diagrammatically in Figure 6. The configuration is as indicated in Figure 7.

The VTEM max Receiver and transmitter coils were in concentric-coplanar and Z-direction oriented configuration. The receiver system for the project also included a coincident-coaxial X-direction coil to measure the in-line dB/dt and calculate B-Field responses. The EM transmitter-receiver loop was towed at a mean distance of 48 metres below the aircraft as shown in Figure 7.

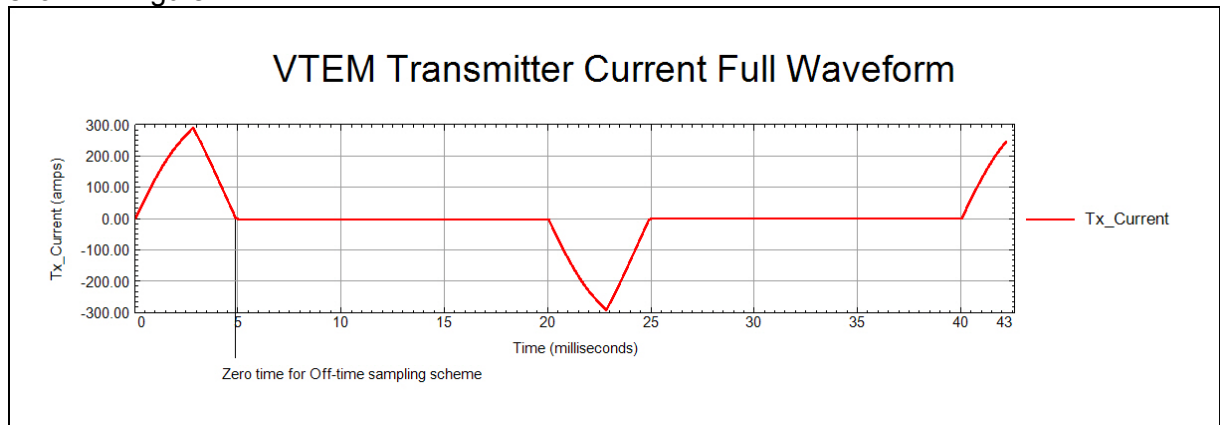


Figure 6: VTEM Transmitter Current Waveform

The VTEM decay sampling scheme is shown in Table 3 below. Forty four time measurement gates were used for the final data processing in the range from 0.031 to 12.250 msec. Zero time for the off-time sampling scheme is equal to the current pulse width and is defined as the time near the end of the turn-off ramp where the di/dt waveform falls to 1/2 of its peak value.

Table 3: Off-Time Decay Sampling Scheme

VTEM Decay Sampling Scheme				
index	Start	End	Middle	Width
Miliseconds				
6	0.029	0.034	0.031	0.005
7	0.034	0.039	0.036	0.005
8	0.039	0.045	0.042	0.006
9	0.045	0.051	0.048	0.007
10	0.051	0.059	0.055	0.008
11	0.059	0.068	0.063	0.009
12	0.068	0.078	0.073	0.010
13	0.078	0.090	0.083	0.012
14	0.090	0.103	0.096	0.013
15	0.103	0.118	0.110	0.015
16	0.118	0.136	0.126	0.018
17	0.136	0.156	0.145	0.020
18	0.156	0.179	0.167	0.023
19	0.179	0.206	0.192	0.027
20	0.206	0.236	0.220	0.030
21	0.236	0.271	0.253	0.035
22	0.271	0.312	0.290	0.040
23	0.312	0.358	0.333	0.046
24	0.358	0.411	0.383	0.053
25	0.411	0.472	0.440	0.061
26	0.472	0.543	0.505	0.070
27	0.543	0.623	0.580	0.081
28	0.623	0.716	0.667	0.093
29	0.716	0.823	0.766	0.107
30	0.823	0.945	0.880	0.122
31	0.945	1.086	1.010	0.141
32	1.086	1.247	1.161	0.161
33	1.247	1.432	1.333	0.185
34	1.432	1.646	1.531	0.214
35	1.646	1.891	1.760	0.245
36	1.891	2.172	2.021	0.281
37	2.172	2.495	2.323	0.323
38	2.495	2.865	2.667	0.370
39	2.865	3.292	3.063	0.427

VTEM Decay Sampling Scheme				
index	Start	End	Middle	Width
Miliseconds				
40	3.292	3.781	3.521	0.490
41	3.781	4.341	4.042	0.560
42	4.341	4.987	4.641	0.646
43	4.987	5.729	5.333	0.742
44	5.729	6.581	6.125	0.852
45	6.581	7.560	7.036	0.979
46	7.560	8.685	8.083	1.125
47	8.685	9.977	9.286	1.292
48	9.977	11.458	10.667	1.482
49	11.458	13.161	12.250	1.703

Z Component: 6 - 49 time gates
X Component: 20 - 49 time gates.

VTEM max system specification:

Transmitter

- Transmitter loop diameter: 35 m
- Effective Transmitter loop area: 3848 m²
- Number of turns: 4
- Transmitter base frequency: 25 Hz
- Peak current: 293 A
- Pulse width: 4.92 ms
- Wave form shape: trapezoid
- Peak dipole moment: 1,119,768 nIA
- Actual average EM Transmitter-receiver loop terrain clearance: 42 metres above the ground

Receiver

- X Coil diameter: 0.32 m
- Number of turns: 245
 - Effective coil area: 19.69 m²
 - Z-Coil diameter: 1.2 m
 - Number of turns: 100
 - Effective coil area: 113.04 m²

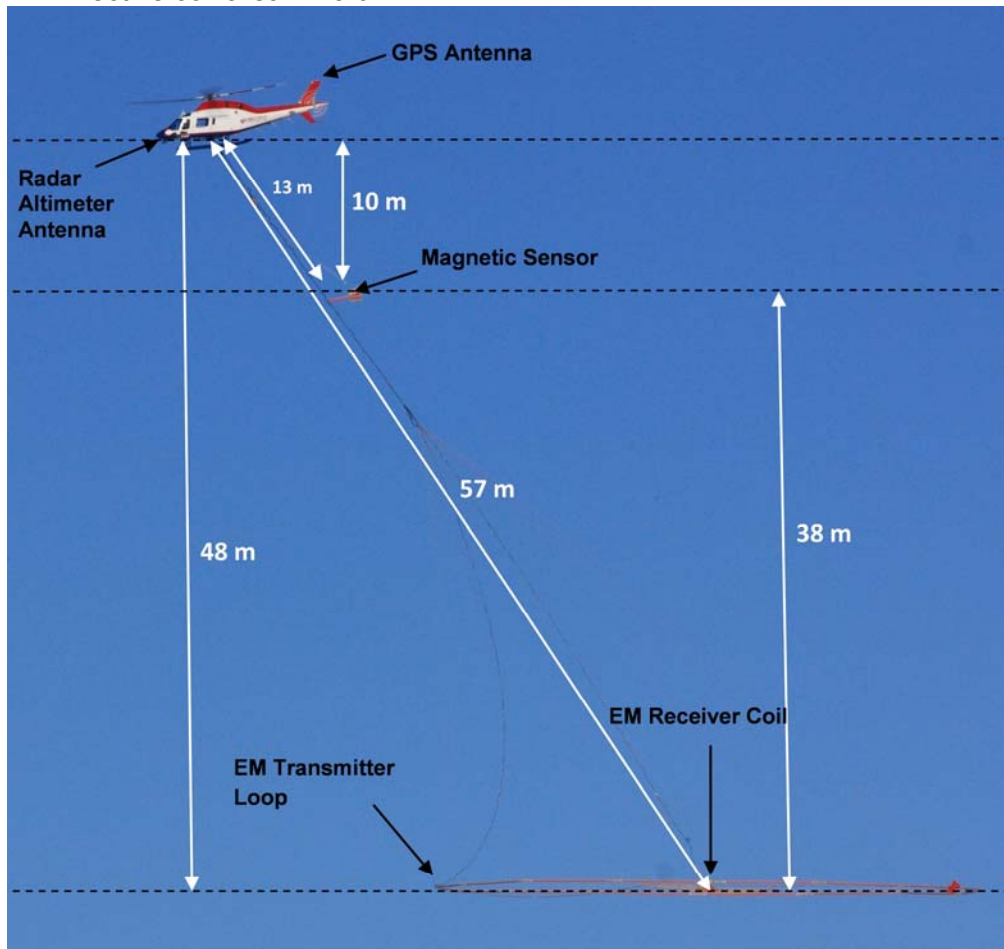


Figure 7: VTEM max System Configuration.

2.4.3 Airborne magnetometer

The magnetic sensor utilized for the survey was Geometrics optically pumped caesium vapour magnetic field sensor mounted 10 metres below the helicopter, as shown in Figure 7. The sensitivity of the magnetic sensor is 0.02 nanoTesla (nT) at a sampling interval of 0.1 seconds.

2.4.4 FULL WAVEFORM VTEM Sensor Calibration

The calibration is performed on the complete VTEM system installed in and connected to the helicopter, using special calibration equipment.

The procedure takes half-cycle files acquired and calculates a calibration file consisting of a single stacked half-cycle waveform. The purpose of the stacking is to attenuate natural and man-made magnetic signals, leaving only the response to the calibration signal.

2.4.5 Radar Altimeter

A Terra TRA 3000/TRI 40 radar altimeter was used to record terrain clearance. The antenna was mounted beneath the bubble of the helicopter cockpit (Figure 7).

2.4.6 GPS Navigation System

The navigation system used was a Geotech PC104 based navigation system utilizing a NovAtel's WAAS (Wide Area Augmentation System) enabled GPS receiver, Geotech navigate software, a full screen display with controls in front of the pilot to direct the flight and a NovAtel GPS antenna mounted on the helicopter tail (Figure 7). As many as 11 GPS and two WAAS satellites may be monitored at any one time. The positional accuracy or circular error probability (CEP) is 1.8 m, with WAAS active, it is 1.0 m. The co-ordinates of the block were set-up prior to the survey and the information was fed into the airborne navigation system.

2.4.7 Digital Acquisition System

A Geotech data acquisition system recorded the digital survey data on an internal compact flash card. Data is displayed on an LCD screen as traces to allow the operator to monitor the integrity of the system. The data type and sampling interval as provided in Table 4.

Table 4: Acquisition Sampling Rates

Data Type	Sampling
TDEM	0.1 sec
Magnetometer	0.1 sec
GPS Position	0.2 sec
Radar Altimeter	0.2 sec

2.5 Base Station

A combined magnetometer/GPS base station was utilized on this project. A Geometrics Caesium vapour magnetometer was used as a magnetic sensor with a sensitivity of 0.001 nT. The base station was recording the magnetic field together with the GPS time at 1 Hz on a base station computer.

The base station magnetometer sensor was installed near the Myra Camp (12° 27.4477' S, 133° 17.0696' E); away from electric transmission lines and moving ferrous objects such as motor vehicles. The base station data were backed-up to the data processing computer at the end of each survey day.

3. PERSONNEL

The following Geotech Ltd. personnel were involved in the project.

Field:

Project Manager:	Leon Lovelock (Office)
Data QC:	Nick Venter (Office)
Crew chief:	Jono Gray
Operator:	Paul White

The survey pilot and the mechanical engineer were employed directly by the helicopter operator – United Aero Helicopters.

Pilot:	Mark Loghridge
--------	----------------

Office:

Preliminary Data Processing:	Nick Venter
Final Data Processing:	TaiChyi Shei
Final Data QA/QC:	Geoffrey Plastow
Reporting/Mapping:	Wendy Acorn

Data acquisition phase was carried out under the supervision of Andrei Bagrianski, P. Geo, Chief Operating Officer. The processing and interpretation phase was under the supervision of Geoffrey Plastow, P. Geo Data Processing Manager. The customer relations were looked after by Keith Fisk.

4. DATA PROCESSING AND PRESENTATION

Data compilation and processing were carried out by the application of Geosoft OASIS Montaj and programs proprietary to Geotech Ltd.

4.1 Flight Path

The flight path, recorded by the acquisition program as WGS 84 latitude/longitude, was converted into the GDA94, Map Grid of Australia zone 53 coordinate system in Oasis Montaj.

The flight path was drawn using linear interpolation between x, y positions from the navigation system. Positions are updated every second and expressed as UTM easting's (x) and UTM northing's (y).

4.2 Electromagnetic Data

The Full Waveform EM specific data processing operations included:

- Half cycle stacking (performed at time of acquisition);
- System response correction;
- Parasitic and drift removal.

A three stage digital filtering process was used to reject major sferic events and to reduce system noise. Local sferic activity can produce sharp, large amplitude events that cannot be removed by conventional filtering procedures. Smoothing or stacking will reduce their amplitude but leave a broader residual response that can be confused with geological phenomena. To avoid this possibility, a computer algorithm searches out and rejects the major sferic events.

The signal to noise ratio was further improved by the application of a low pass linear digital filter. This filter has zero phase shift which prevents any lag or peak displacement from occurring, and it suppresses only variations with a wavelength less than about 1 second or 15 metres. This filter is a symmetrical 1 sec linear filter.

The results are presented as stacked profiles of EM voltages for the time gates, in linear - logarithmic scale for the B-field Z component and dB/dt responses in the Z and X components. B-field Z component time channel recorded at 0.505 milliseconds after the termination of the impulse is also presented as contour colour images. Fraser Filter X component is also presented as a colour image. Calculated Time Constant (TAU) with Calculated Vertical Derivative contours is presented in Appendix C and E. Resistivity Depth Image (RDI) is also presented in Appendix F and G.

VTEM max has two receiver coil orientations. Z-axis coil is oriented parallel to the transmitter coil axis and both are horizontal to the ground. The X-axis coil is oriented parallel to the ground and along the line-of-flight. This combined two coil configuration provides information on the position, depth, dip and thickness of a conductor. Generalized modeling results of VTEM max data are shown in Appendix D.

In general X-component data produce cross-over type anomalies: from “+ to –” in flight direction of flight for “thin” sub vertical targets and from “- to +” in direction of flight for “thick” targets. Z component data produce double peak type anomalies for “thin” sub vertical targets and single peak for “thick” targets.

The limits and change-over of “thin-thick” depends on dimensions of a TEM system.

Because of X component polarity is under line-of-flight, convolution Fraser filter (FF, Figure 8) is applied to X component data to represent axes of conductors in the form of grid map. In this case positive FF anomalies always correspond to “plus-to-minus” X data crossovers independently of direction of flight.

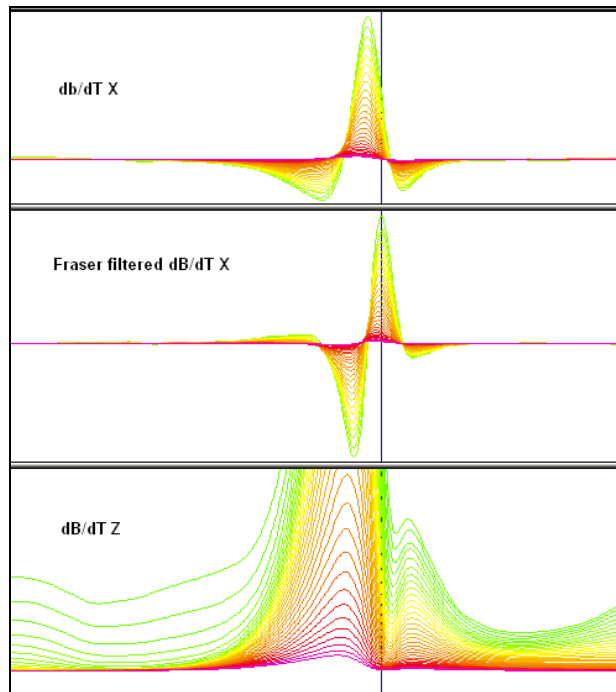


Figure 8: Z, X and Fraser filtered X (FFx) components for “thin” target.

4.3 Magnetic Data

The processing of the magnetic data involved the correction for diurnal variations by using the digitally recorded ground base station magnetic values. The base station magnetometer data was edited and merged into the Geosoft GDB database on a daily basis. The aeromagnetic data was corrected for diurnal variations by subtracting the observed magnetic base station deviations.

The corrected magnetic data was interpolated between survey lines using a random point gridding method to yield x-y grid values for a standard grid cell size of approximately 50 metres at the mapping scale. The Minimum Curvature algorithm was used to interpolate values onto a rectangular regular spaced grid.

5. DELIVERABLES

5.1 Survey Report

The survey report describes the data acquisition, processing, and final presentation of the survey results. The survey report is provided in two paper copies and digitally in PDF format.

5.2 Maps

Final maps were produced at a scale of 1:20,000 for best representation of the survey size and line spacing. The coordinate/projection system used was GDA94 Datum, Map Grid of Australia zone 53. All maps show the flight path trace and topographic data; latitude and longitude are also noted on maps.

The preliminary and final results of the survey are presented as EM profiles, a late-time gate gridded EM channel, and a colour magnetic TMI contour map.

- Maps at 1:20,000 in Geosoft MAP format, as follows:

AA140346_20k_dBdt:	dB/dt profiles Z Component, Time Gates 0.220 – 7.036 ms in linear – logarithmic scale.
AA140346_20k_Bfield:	B-field profiles Z Component, Time Gates 0.220 – 7.036 ms in linear – logarithmic scale over Total Magnetic Intensity
AA140346_20k_BFz36:	B-field late time Z Component Channel 36, Time Gate 2.021 ms
AA140346_20k_TMI:	Total Magnetic Intensity (TMI)
AA140346_20k_SFxFF26:	Fraser Filtered dB/dt X Component, Channel 26, Time Gate 0.505 ms
AA140346_20k_TauSF:	dB/dt Calculated Time Constant (TAU) with Calculated Vertical Derivative contours

Maps are also presented in PDF format.

- 1:50,000 topographic vectors were taken from the NRCAN Geogratis database at; <http://geogratis.gc.ca/geogratis/en/index.html>, Australian Government -Geoscience Australia at 1:250,000 scale (www.ga.gov.au) and DIVA-GIS 1:1,000,000 scale data set for Australia (www.diva-gis.org)
- A Google Earth file *AA140346_Alligator.kml* showing the flight path of the block is included. Free versions of Google Earth software from: <http://earth.google.com/download-earth.html>

5.3 Digital Data

- Two copies of the data and maps on DVD were prepared to accompany the report. Each DVD contains a digital file of the line data in GDB Geosoft Montaj and ASEG-GDF format as well as the maps in Geosoft Montaj Map and PDF format.

- DVD structure.

Data	contains databases, grids and maps, as described below.
Report	contains a copy of the report and appendices in PDF format.

Databases in Geosoft GDB format, containing the channels listed in Table 5.

Table 5: Geosoft GDB Data Format

Channel name	Units	Description
X:	metres	Map Grid of Australia zone 53 – GDA94
Y:	metres	Map Grid of Australia zone 53 – GDA94
Longitude:	Decimal Degrees	WGS 84 Longitude data
Latitude:	Decimal Degrees	WGS 84 Latitude data
Z:	metres	GPS antenna elevation (above Geoid)
Zb:	metres	Transmitter-receiver loop elevation (above Geoid)
Radar:	metres	helicopter terrain clearance from radar altimeter
Radarb:	metres	Calculated EM transmitter-receiver loop terrain clearance from radar altimeter
DEM:	metres	Digital Elevation Model
Gtime:	Seconds of the day	GPS time
Mag1:	nT	Raw Total Magnetic field data
Basemag:	nT	Magnetic diurnal variation data
Mag2:	nT	Diurnal corrected Total Magnetic field data
TMI:	nT	Levelled Total Magnetic field data
CVG	nT/m	Calculated Vertical Derivative
SFz[6]:	$pV/(A*m^4)$	Z dB/dt 0.031 millisecond time channel
SFz[7]:	$pV/(A*m^4)$	Z dB/dt 0.036 millisecond time channel
SFz[8]:	$pV/(A*m^4)$	Z dB/dt 0.042 millisecond time channel
SFz[9]:	$pV/(A*m^4)$	Z dB/dt 0.048 millisecond time channel
SFz[10]:	$pV/(A*m^4)$	Z dB/dt 0.055 millisecond time channel
SFz[11]:	$pV/(A*m^4)$	Z dB/dt 0.063 millisecond time channel
SFz[12]:	$pV/(A*m^4)$	Z dB/dt 0.073 millisecond time channel
SFz[13]:	$pV/(A*m^4)$	Z dB/dt 0.083 millisecond time channel
SFz[14]:	$pV/(A*m^4)$	Z dB/dt 0.096 millisecond time channel
SFz[15]:	$pV/(A*m^4)$	Z dB/dt 0.110 millisecond time channel
SFz[16]:	$pV/(A*m^4)$	Z dB/dt 0.126 millisecond time channel
SFz[17]:	$pV/(A*m^4)$	Z dB/dt 0.145 millisecond time channel
SFz[18]:	$pV/(A*m^4)$	Z dB/dt 0.167 millisecond time channel
SFz[19]:	$pV/(A*m^4)$	Z dB/dt 0.192 millisecond time channel
SFz[20]:	$pV/(A*m^4)$	Z dB/dt 0.220 millisecond time channel
SFz[21]:	$pV/(A*m^4)$	Z dB/dt 0.253 millisecond time channel
SFz[22]:	$pV/(A*m^4)$	Z dB/dt 0.290 millisecond time channel
SFz[23]:	$pV/(A*m^4)$	Z dB/dt 0.333 millisecond time channel
SFz[24]:	$pV/(A*m^4)$	Z dB/dt 0.383 millisecond time channel
SFz[25]:	$pV/(A*m^4)$	Z dB/dt 0.440 millisecond time channel
SFz[26]:	$pV/(A*m^4)$	Z dB/dt 0.505 millisecond time channel
SFz[27]:	$pV/(A*m^4)$	Z dB/dt 0.580 millisecond time channel
SFz[28]:	$pV/(A*m^4)$	Z dB/dt 0.667 millisecond time channel
SFz[29]:	$pV/(A*m^4)$	Z dB/dt 0.766 millisecond time channel
SFz[30]:	$pV/(A*m^4)$	Z dB/dt 0.880 millisecond time channel
SFz[31]:	$pV/(A*m^4)$	Z dB/dt 1.010 millisecond time channel
SFz[32]:	$pV/(A*m^4)$	Z dB/dt 1.161 millisecond time channel
SFz[33]:	$pV/(A*m^4)$	Z dB/dt 1.333 millisecond time channel
SFz[34]:	$pV/(A*m^4)$	Z dB/dt 1.531 millisecond time channel

Channel name	Units	Description
SFz[35]:	pV/(A*m ⁴)	Z dB/dt 1.760 millisecond time channel
SFz[36]:	pV/(A*m ⁴)	Z dB/dt 2.021 millisecond time channel
SFz[37]:	pV/(A*m ⁴)	Z dB/dt 2.323 millisecond time channel
SFz[38]:	pV/(A*m ⁴)	Z dB/dt 2.667 millisecond time channel
SFz[39]:	pV/(A*m ⁴)	Z dB/dt 3.063 millisecond time channel
SFz[40]:	pV/(A*m ⁴)	Z dB/dt 3.521 millisecond time channel
SFz[41]:	pV/(A*m ⁴)	Z dB/dt 4.042 millisecond time channel
SFz[42]:	pV/(A*m ⁴)	Z dB/dt 4.641 millisecond time channel
SFz[43]:	pV/(A*m ⁴)	Z dB/dt 5.333 millisecond time channel
SFz[44]:	pV/(A*m ⁴)	Z dB/dt 6.125 millisecond time channel
SFz[45]:	pV/(A*m ⁴)	Z dB/dt 7.036 millisecond time channel
SFz[46]:	pV/(A*m ⁴)	Z dB/dt 8.083 millisecond time channel
SFz[47]:	pV/(A*m ⁴)	Z dB/dt 9.286 millisecond time channel
SFz[48]:	pV/(A*m ⁴)	Z dB/dt 10.667 millisecond time channel
SFz[49]:	pV/(A*m ⁴)	Z dB/dt 12.250 millisecond time channel
SFx[20]:	pV/(A*m ⁴)	X dB/dt 0.220 millisecond time channel
SFx[21]:	pV/(A*m ⁴)	X dB/dt 0.253 millisecond time channel
SFx[22]:	pV/(A*m ⁴)	X dB/dt 0.290 millisecond time channel
SFx[23]:	pV/(A*m ⁴)	X dB/dt 0.333 millisecond time channel
SFx[24]:	pV/(A*m ⁴)	X dB/dt 0.383 millisecond time channel
SFx[25]:	pV/(A*m ⁴)	X dB/dt 0.440 millisecond time channel
SFx[26]:	pV/(A*m ⁴)	X dB/dt 0.505 millisecond time channel
SFx[27]:	pV/(A*m ⁴)	X dB/dt 0.580 millisecond time channel
SFx[28]:	pV/(A*m ⁴)	X dB/dt 0.667 millisecond time channel
SFx[29]:	pV/(A*m ⁴)	X dB/dt 0.766 millisecond time channel
SFx[30]:	pV/(A*m ⁴)	X dB/dt 0.880 millisecond time channel
SFx[31]:	pV/(A*m ⁴)	X dB/dt 1.010 millisecond time channel
SFx[32]:	pV/(A*m ⁴)	X dB/dt 1.161 millisecond time channel
SFx[33]:	pV/(A*m ⁴)	X dB/dt 1.333 millisecond time channel
SFx[34]:	pV/(A*m ⁴)	X dB/dt 1.531 millisecond time channel
SFx[35]:	pV/(A*m ⁴)	X dB/dt 1.760 millisecond time channel
SFx[36]:	pV/(A*m ⁴)	X dB/dt 2.021 millisecond time channel
SFx[37]:	pV/(A*m ⁴)	X dB/dt 2.323 millisecond time channel
SFx[38]:	pV/(A*m ⁴)	X dB/dt 2.667 millisecond time channel
SFx[39]:	pV/(A*m ⁴)	X dB/dt 3.063 millisecond time channel
SFx[40]:	pV/(A*m ⁴)	X dB/dt 3.521 millisecond time channel
SFx[41]:	pV/(A*m ⁴)	X dB/dt 4.042 millisecond time channel
SFx[42]:	pV/(A*m ⁴)	X dB/dt 4.641 millisecond time channel
SFx[43]:	pV/(A*m ⁴)	X dB/dt 5.333 millisecond time channel
SFx[44]:	pV/(A*m ⁴)	X dB/dt 6.125 millisecond time channel
SFx[45]:	pV/(A*m ⁴)	X dB/dt 7.036 millisecond time channel
SFx[46]:	pV/(A*m ⁴)	X dB/dt 8.083 millisecond time channel
SFx[47]:	pV/(A*m ⁴)	X dB/dt 9.286 millisecond time channel
SFx[48]:	pV/(A*m ⁴)	X dB/dt 10.667 millisecond time channel
SFx[49]:	pV/(A*m ⁴)	X dB/dt 12.250 millisecond time channel
BFz	(pV*ms)/(A*m ⁴)	Z B-Field data for time channels 6 to 49
BFx	(pV*ms)/(A*m ⁴)	X B-Field data for time channels 20 to 49
SFxFF	pV/(A*m ⁴)	Fraser filtered X dB/dt
TauSF	milliseconds	Time Constant (Tau) calculated from dB/dt data
NchanSF		Last channel where the algorithm stops calculation, dB/dt

Channel name	Units	Description
TauBF	milliseconds	Time Constant (Tau) calculated from B-field data
NchanBF		Last channel where the algorithm stops calculation, B-Field
PLM:		50 Hz power line monitor

Electromagnetic B-field and dB/dt Z component data is found in array channel format between indexes 6 – 49, and X component data from 20 – 49, as described above.

- Database of the Resistivity Depth Images in Geosoft GDB format, containing the following channels:

Table 6: Geosoft Resistivity Depth Image GDB Data Format

Channel name	Units	Description
Xg	metres	Map Grid of Australia zone 53 – GDA94
Yg	metres	Map Grid of Australia zone 53 – GDA94
Dist:	meters	Distance from the beginning of the line
Depth:	meters	array channel, depth from the surface
Z:	meters	array channel, depth from sea level
AppRes:	Ohm-m	array channel, Apparent Resistivity
TR:	meters	EM system height from sea level
Topo:	meters	digital elevation model
Radarb:	metres	Calculated Transmitter-receiver loop terrain clearance from radar altimeter
SF:	pV/(A*m ⁴)	array channel, dB/dT
MAG:	nT	TMI data
CVG:	nT/m	CVG data
DOI:	metres	Depth of Investigation: a measure of VTEM depth effectiveness
PLM:		60Hz Power Line Monitor

- Database of the VTEM Waveform “AA140346_waveform_final.gdb” in Geosoft GDB format, containing the following channels:

Table 7: Geosoft database for the VTEM waveform

Channel name	Description
Time:	Sampling rate interval, 5.2083 microseconds
Tx Current:	Output current of the transmitter

- Grids in Geosoft GRD, ER Mapper and GeoTIFF format, as follows:
 - BFz26: B-Field Z Component Channel 26 (Time Gate 0.505 ms)
 - SFz12: dB/dt Z Component Channel 12 (Time Gate 0.073 ms)
 - SFz28: dB/dt Z Component Channel 28 (Time Gate 0.667 ms)
 - SFz40: dB/dt Z Component Channel 40 (Time Gate 3.521 ms)
 - TMI: Total Magnetic Intensity (nT)
 - CVG: Calculated Vertical Derivative (nT/m)
 - TauBF: B-Field Calculated Time Constant (ms)
 - TauSF: dB/dt Calculated Time Constant (ms)
 - SFxFF26: Fraser Filter X Component dB/dt Channel 26 (Time Gate 0.505 ms)

DEM: Digital Elevation Model (metres)

A Geosoft .GRD file has a .GI metadata file associated with it, containing grid projection information. A grid cell size of 50 metres was used.

6. CONCLUSIONS AND RECOMMENDATIONS

A helicopter-borne versatile time domain electromagnetic (VTEM max) geophysical survey has been completed over the Mamadawerre Project blocks Northwest, East 1 and East 2 near Jabiru NT, Australia.

The total area coverage for all properties is 111 km². Total survey line coverage is 533 line kilometres. The principal sensors included a Time Domain EM system and a magnetometer. Results have been presented as stacked profiles, and contour colour images at a scale of 1:20,000. No formal Interpretation has been included.

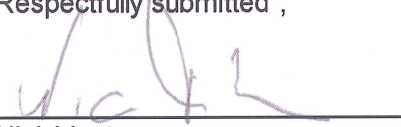
Based on the geophysical results obtained, a number of TEM anomalous zones are identified across the properties. They can be seen overlapping the TAU decay parameter image presented with the calculated vertical magnetic gradient (CVG) contours (see Appendix C).

Overall the conductive zones are associated with the magnetic anomalies in the survey areas. According to apparent resistivity depth images over all lines in all blocks (See Appendix G), the top of the conductive zones is very near surface (approximately less than 50 meters).

In the East 1 Block, the structure of the EM data closely follows the trends in the magnetics data. The apparent resistivity of the conductive zones is estimated to be less than 65 Ohm.m. In the East 2 Block, the conductive zones are mainly in the northwest part of the block. The apparent resistivity of the conductive zones is estimated to be less than 120 Ohm.m. In the Northwest Block, the apparent resistivity of the conductive zones is estimated to be less than 120 Ohm.m, and they are in the eastern portion of the survey area. These areas are best visualized in our RDI images presented with the deliverables of this project.

If the conductors correspond to an exploration model on the area it is recommended picking EM anomalies with conductance grading and center localization of the targets, detail resistivity depth imaging and plate modeling with test drill hole parameters planning prior to ground follow up and drill testing. We recommend EM anomaly picking and EM Maxwell modeling for the survey areas.


Respectfully submitted²,



Nick Venter
Geotech Ltd.



TaiChyi Shei
Geotech Ltd.



Geoffrey Plastow, P. Geo.
Data Processing Manager
Geotech Ltd.
January 2015



² Final data processing of the EM and magnetic data were carried out by TaiChyi Shei, under the supervision of Geoffrey Plastow, P. Geo., Data Processing Manager, from the office of Geotech Ltd. in Aurora, Ontario

APPENDIX A

SURVEY AREA LOCATION MAP



Overview of the Survey Blocks

APPENDIX B

SURVEY BLOCK COORDINATES (WGS 84, UTM Zone 53 South)

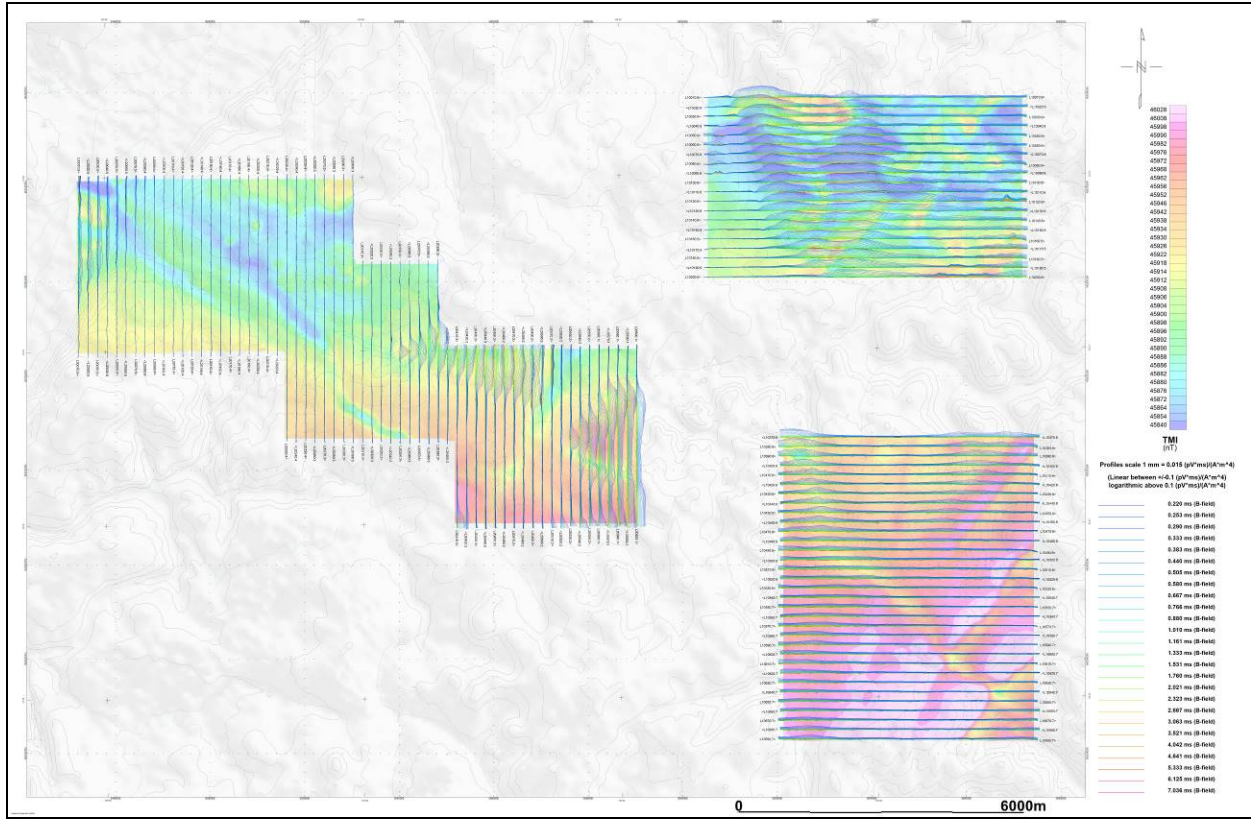
East-1	
X	Y
360583	8633997
367146	8633997
367146	8637937
360583	8637937
360583	8633997

East-2	
X	Y
362167	8624253
367398	8624253
367398	8630755
362167	8630755
362167	8624253

Northwest	
X	Y
347220	8636096
347220	8632520
351420	8632581
351620	8630740
355020	8630701
355220	8628902
359020	8628942
359020	8632520
355020	8632520
354820	8634332
353220	8634291
353020	8636138

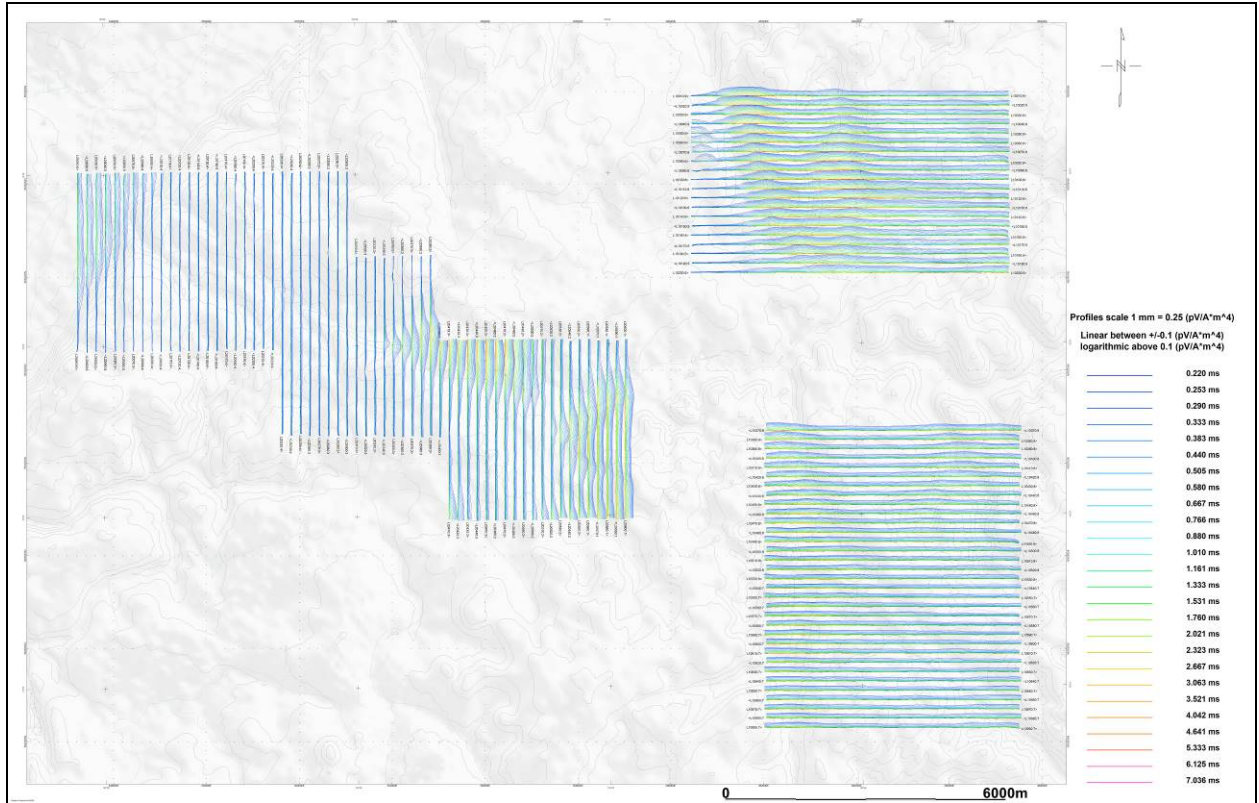
APPENDIX C

GEOPHYSICAL MAPS¹

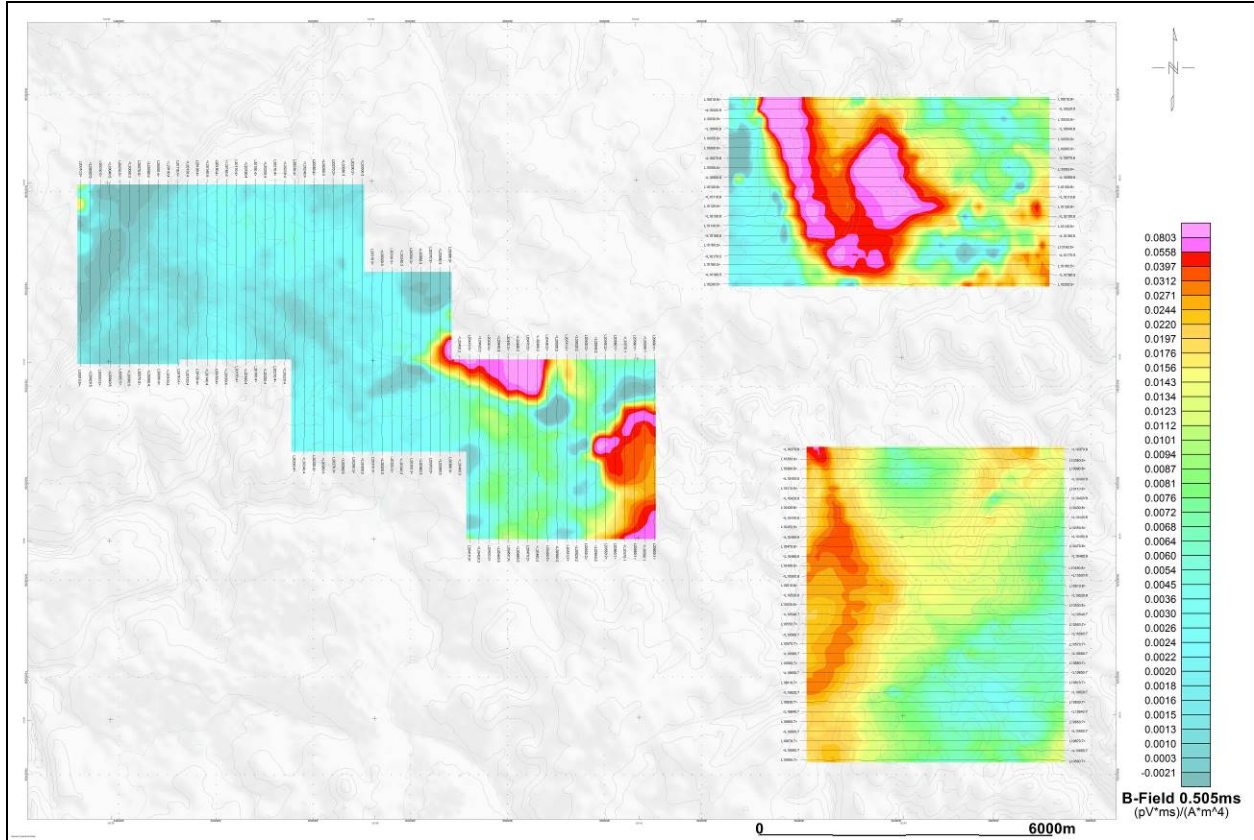


VTEM B-Field Z Component Profiles, Time Gates 0.220 to 7.036 ms

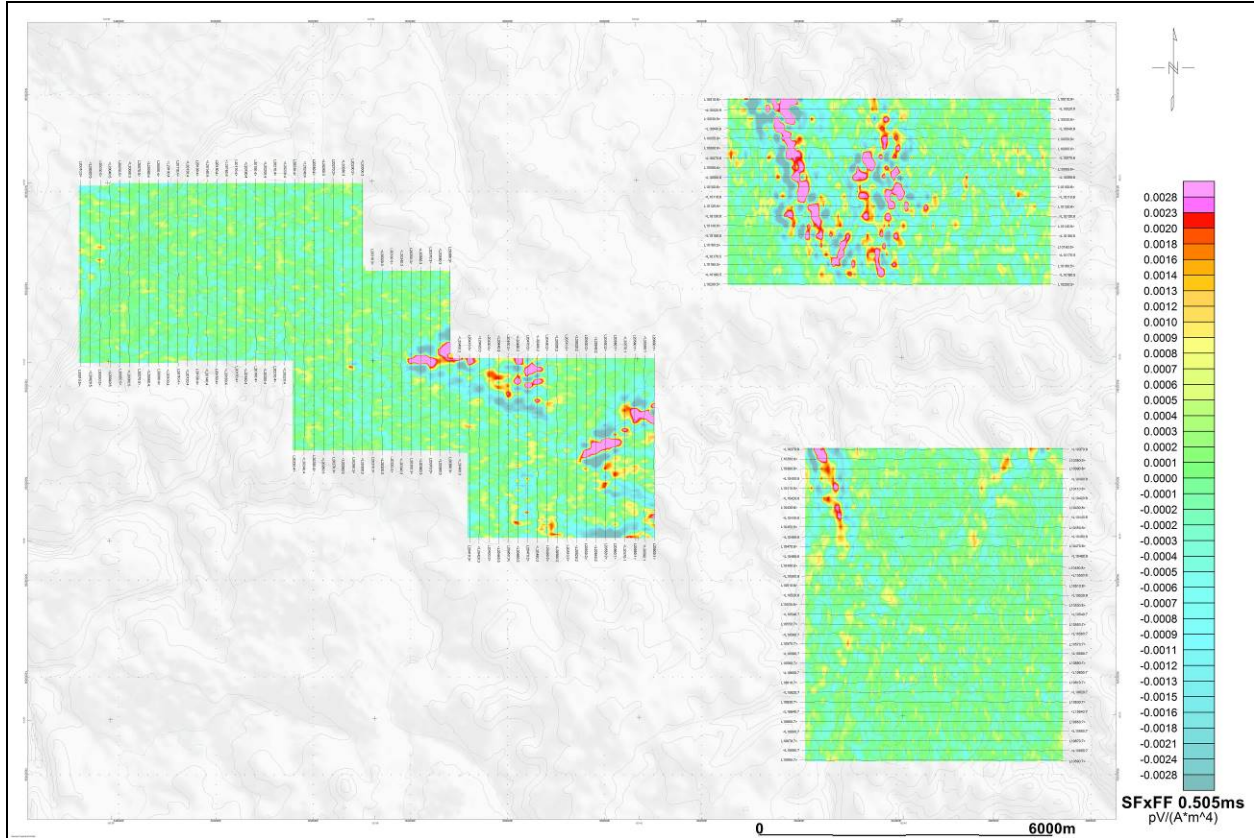
¹ Full size geophysical maps are also available in PDF format on the final DVD



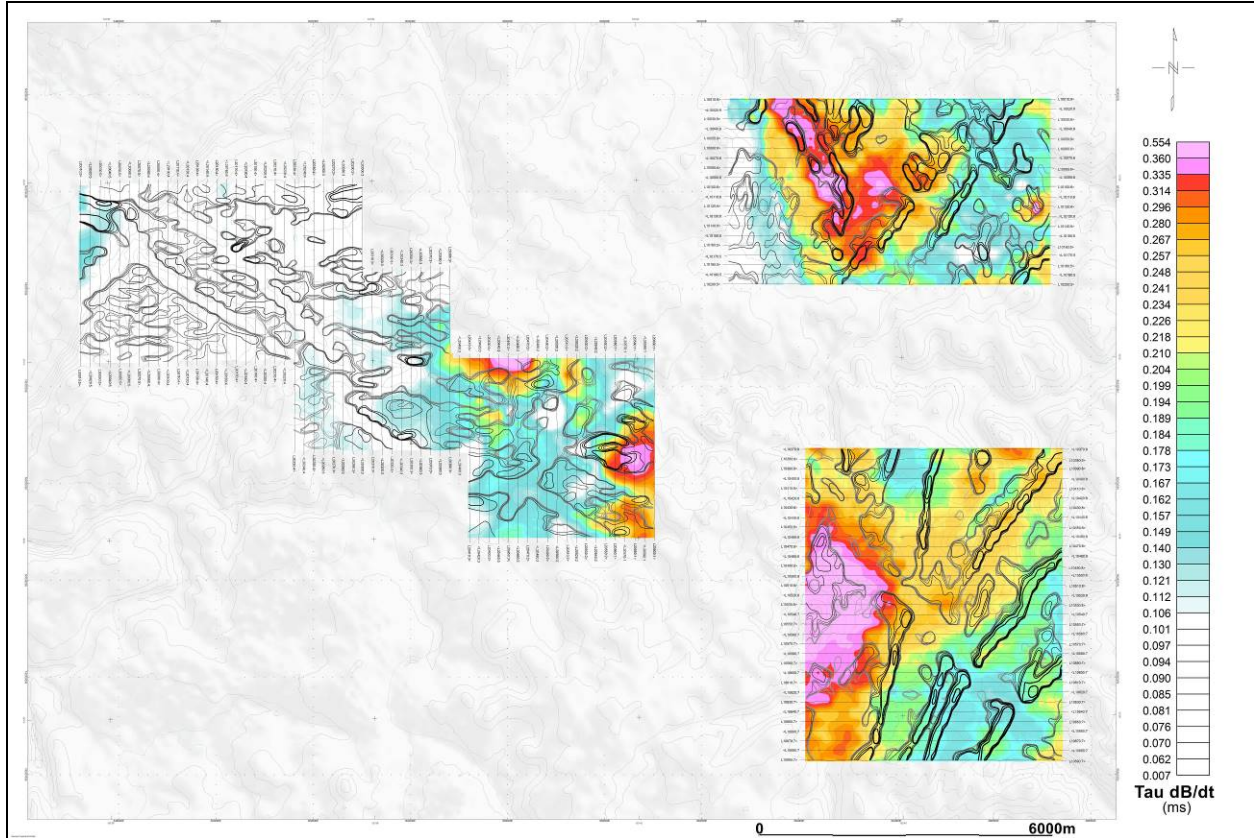
VTEM dB/dt Z Component Profiles, Time Gates 0.220 to 7.036 ms



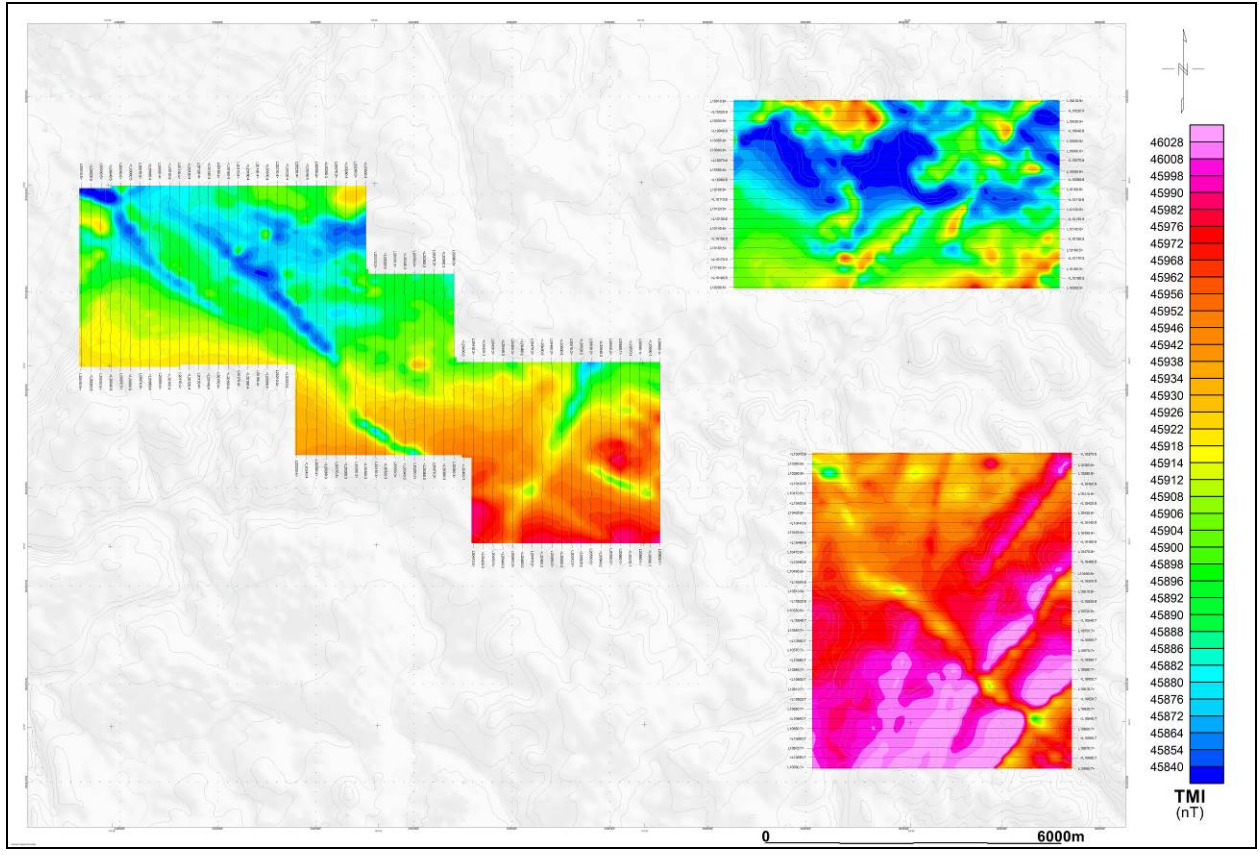
VTEM B-Field Z Component Channel 26, Time Gate 0.505 ms



Fraser Filtered dB/dt X Component Channel 26, Time Gate 0.505 ms

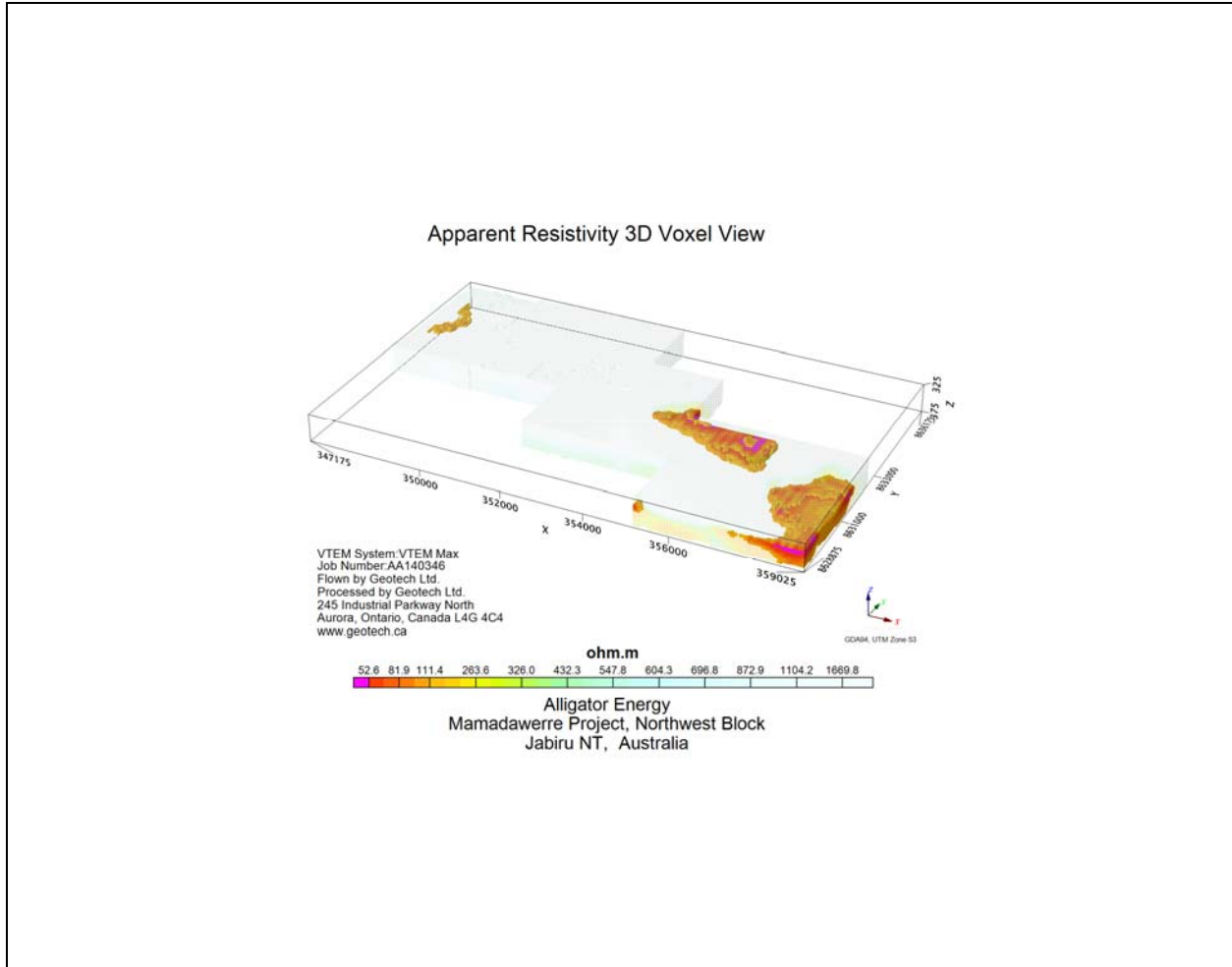


dB/dt Calculated Time Constant (Tau) with Calculated Vertical Derivative contours



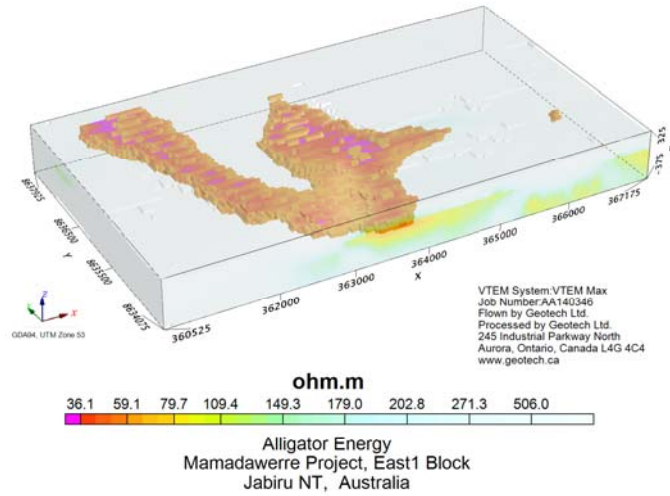
Total Magnetic Intensity (TMI)

RESISTIVITY DEPTH IMAGE (RDI) MAPS



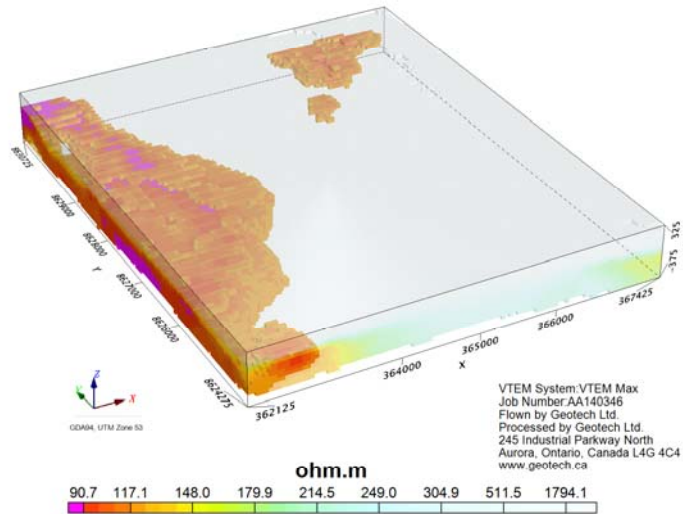
3D Resistivity Depth Images (RDI) – Northwest

Apparent Resistivity 3D Voxel View



3D Resistivity Depth Images (RDI) – East 1

Apparent Resistivity 3D Voxel View



Alligator Energy
Mamadawerre Project, East2 Block
Jabiru NT, Australia

3D Resistivity Depth Images (RDI) – East 2

APPENDIX D

GENERALIZED MODELING RESULTS OF THE VTEM SYSTEM

Introduction

The VTEM system is based on a concentric or central loop design, whereby, the receiver is positioned at the centre of a transmitter loop that produces a primary field. The wave form is a bi-polar, modified square wave with a turn-on and turn-off at each end.

During turn-on and turn-off, a time varying field is produced (dB/dt) and an electro-motive force (emf) is created as a finite impulse response. A current ring around the transmitter loop moves outward and downward as time progresses. When conductive rocks and mineralization are encountered, a secondary field is created by mutual induction and measured by the receiver at the centre of the transmitter loop.

Efficient modeling of the results can be carried out on regularly shaped geometries, thus yielding close approximations to the parameters of the measured targets. The following is a description of a series of common models made for the purpose of promoting a general understanding of the measured results.

A set of models has been produced for the Geotech VTEM® system dB/dT Z and X components (see models D1 to D15). The Maxwell™ modeling program (EMIT Technology Pty. Ltd. Midland, WA, AU) used to generate the following responses assumes a resistive half-space. The reader is encouraged to review these models, so as to get a general understanding of the responses as they apply to survey results. While these models do not begin to cover all possibilities, they give a general perspective on the simple and most commonly encountered anomalies.

As the plate dips and departs from the vertical position, the peaks become asymmetrical.

As the dip increases, the aspect ratio (Min/Max) decreases and this aspect ratio can be used as an empirical guide to dip angles from near 90° to about 30°. The method is not sensitive enough where dips are less than about 30°.

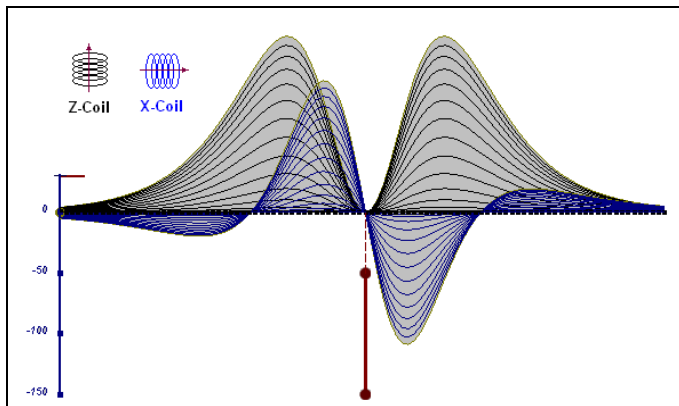


Figure D-1: vertical thin plate

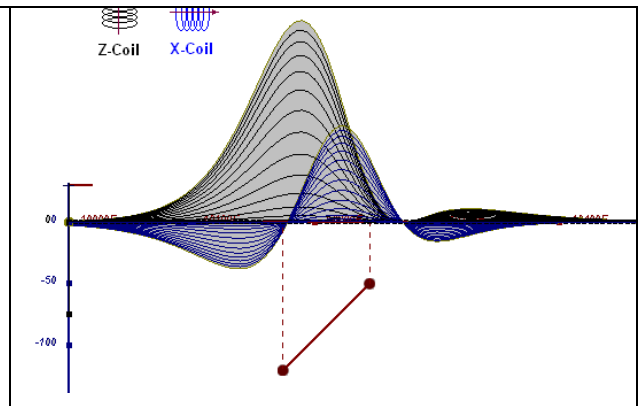


Figure D-2: inclined thin plate

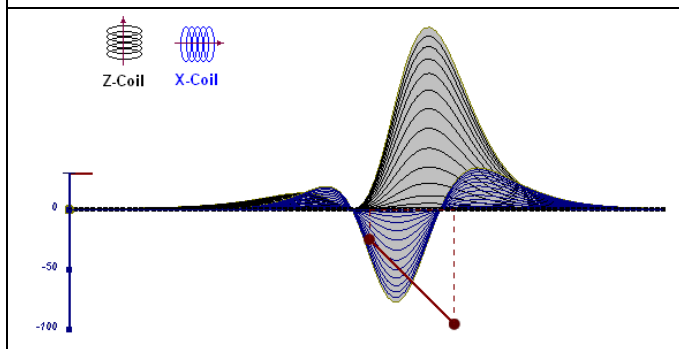


Figure D-3: inclined thin plate

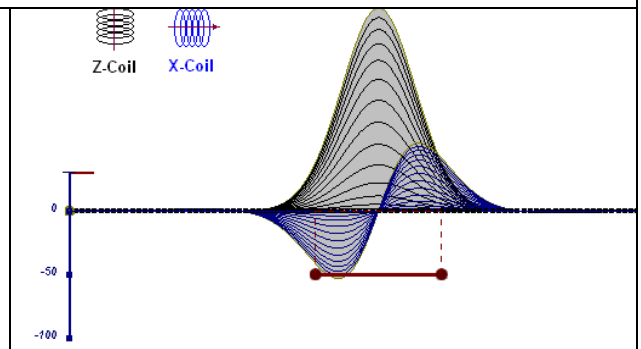


Figure D-4: horizontal thin plate

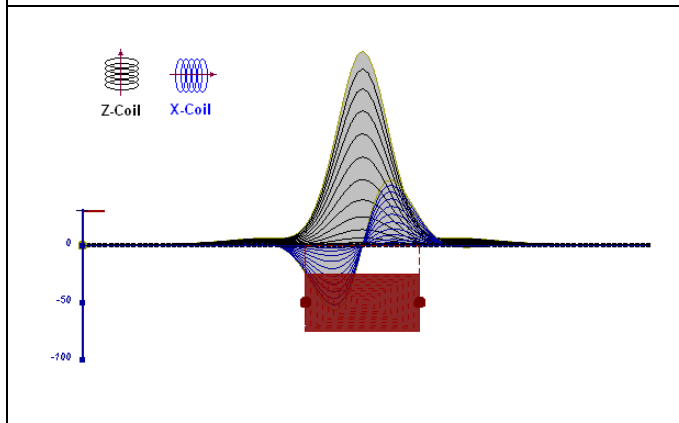


Figure D-5: horizontal thick plate (linear scale of the response)

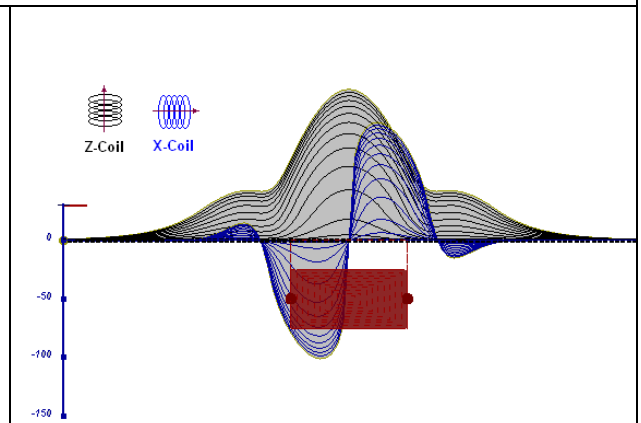


Figure D-6: horizontal thick plate (log scale of the response)

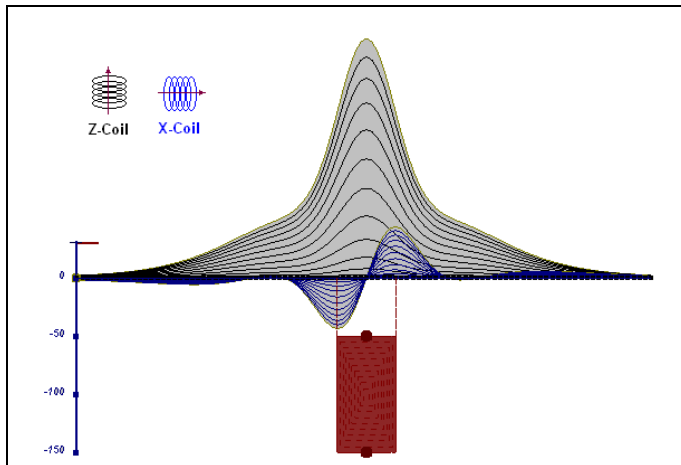


Figure D-7: vertical thick plate (linear scale of the response). 50 m depth

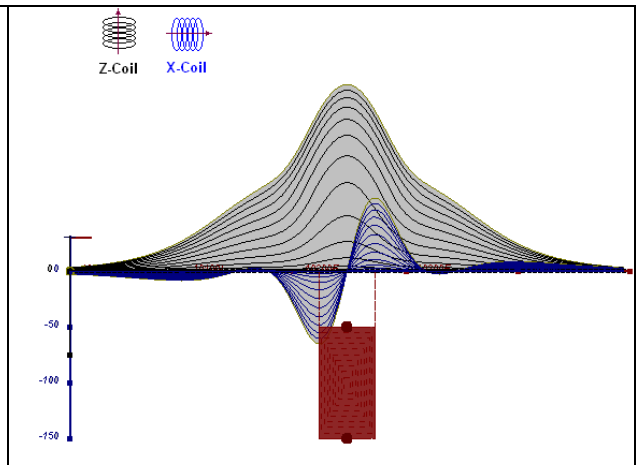


Figure D-8: vertical thick plate (log scale of the response). 50 m depth

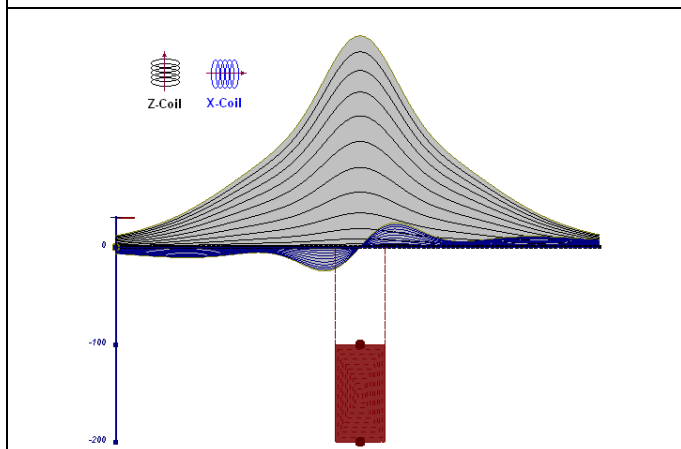


Figure D-9: vertical thick plate (linear scale of the response). 100 m depth

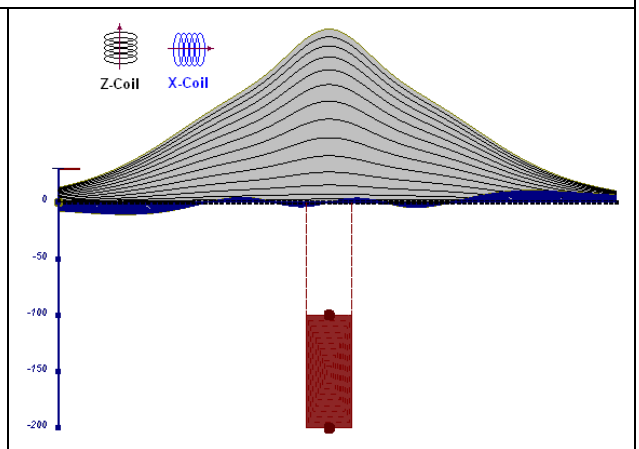


Figure D-10: vertical thick plate (linear scale of the response). Depth/hor.thickness=2.5

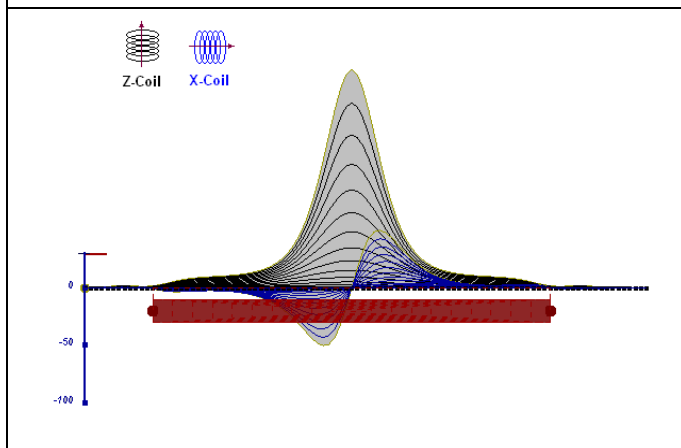


Figure D-10: horizontal thick plate (linear scale of the response)

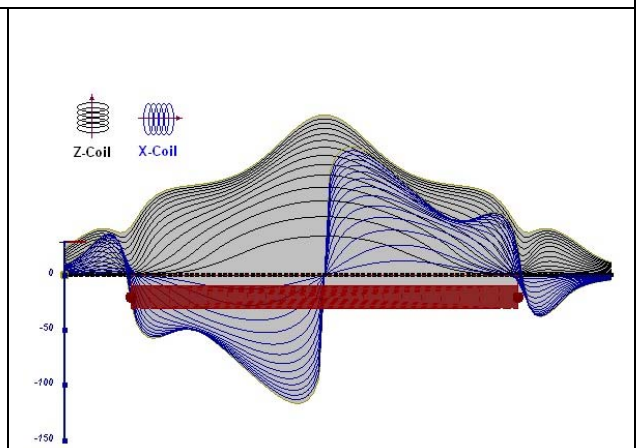


Figure D-11: horizontal thick plate (log scale of the response)

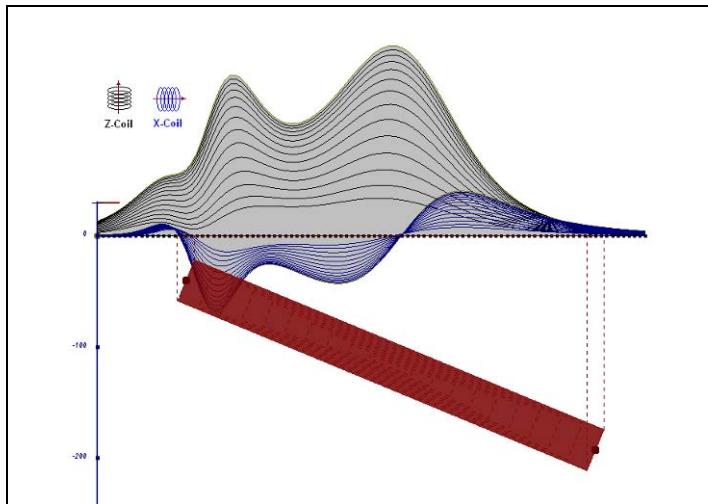


Figure D-12: inclined long thick plate

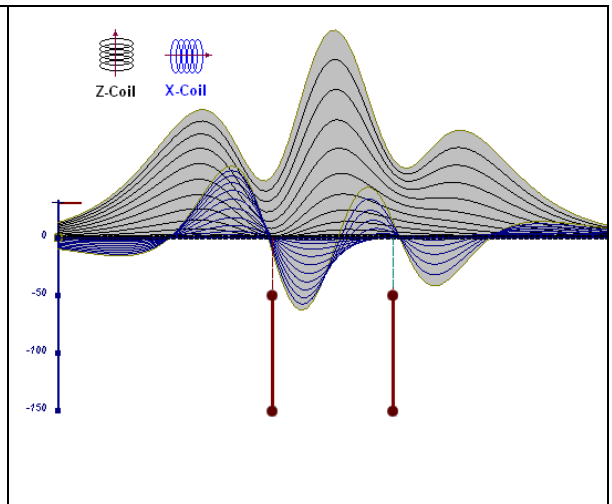


Figure D-13: two vertical thin plates

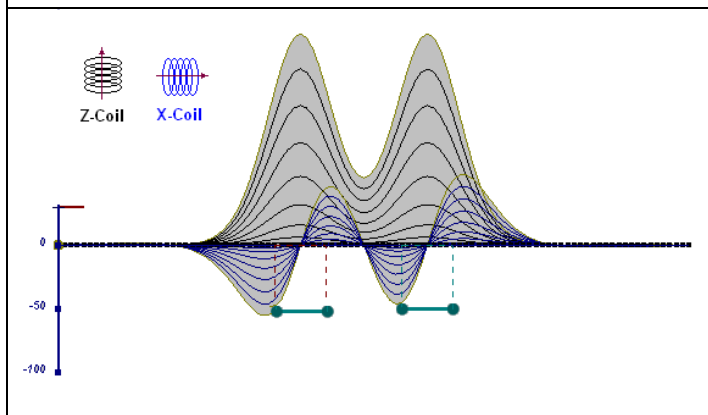


Figure D-14: two horizontal thin plates

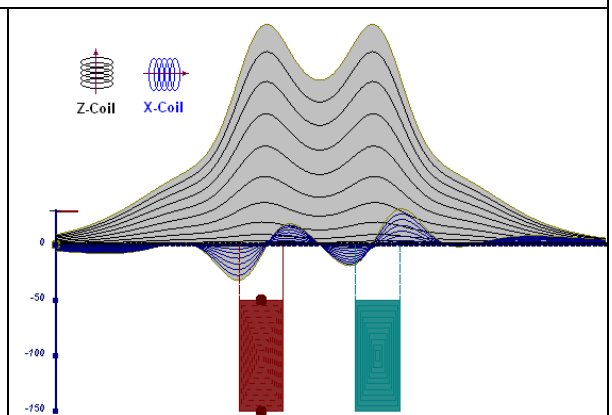


Figure D-15: two vertical thick plates

The same type of target but with different thickness, for example, creates different form of the response:

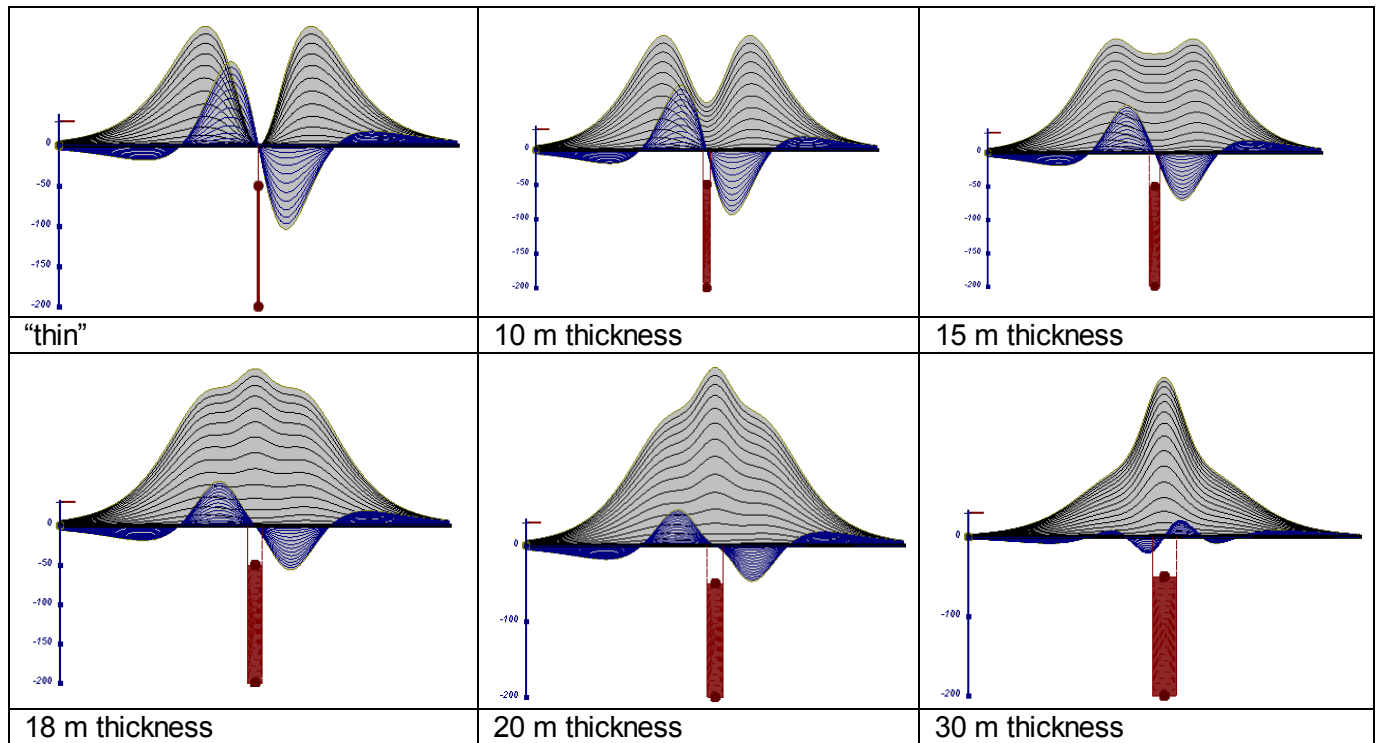


Figure D-16: Conductive vertical plate, depth 50 m, strike length 200 m, depth extend 150 m.

Alexander Prikhodko, PhD, P.Geol
Geotech Ltd.

September 2010

APPENDIX E

EM TIME CONSTANT (TAU) ANALYSIS

Estimation of time constant parameter¹ in transient electromagnetic method is one of the steps toward the extraction of the information about conductances beneath the surface from TEM measurements.

The most reliable method to discriminate or rank conductors from overburden, background or one and other is by calculating the EM field decay time constant (TAU parameter), which directly depends on conductance despite their depth and accordingly amplitude of the response.

Theory

As established in electromagnetic theory, the magnitude of the electro-motive force (emf) induced is proportional to the time rate of change of primary magnetic field at the conductor. This emf causes eddy currents to flow in the conductor with a characteristic transient decay, whose Time Constant (Tau) is a function of the conductance of the survey target or conductivity and geometry (including dimensions) of the target. The decaying currents generate a proportional secondary magnetic field, the time rate of change of which is measured by the receiver coil as induced voltage during the Off time.

The receiver coil output voltage (e_0) is proportional to the time rate of change of the secondary magnetic field and has the form,

$$e_0 \propto (1 / \tau) e^{-(t / \tau)}$$

Where,

$\tau = L/R$ is the characteristic time constant of the target (TAU)

R = resistance

L = inductance

From the expression, conductive targets that have small value of resistance and hence large value of τ yield signals with small initial amplitude that decays relatively slowly with progress of time. Conversely, signals from poorly conducting targets that have large resistance value and small τ , have high initial amplitude but decay rapidly with time¹ (Figure E-1).

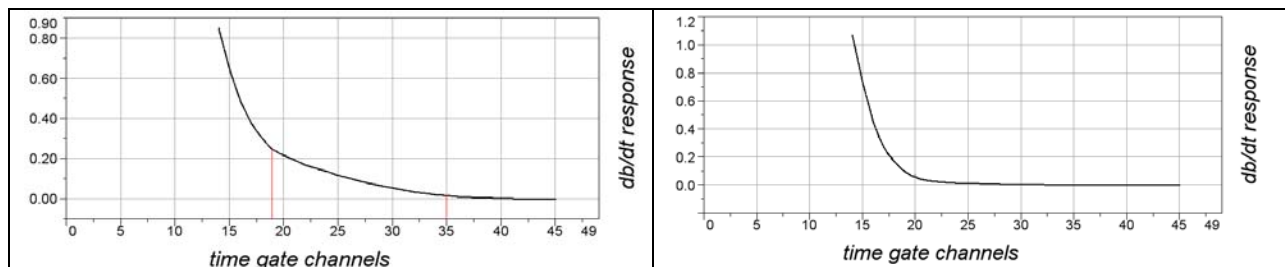


Figure E-1: Left – presence of good conductor, right – poor conductor.

¹ McNeill, JD, 1980, "Applications of Transient Electromagnetic Techniques", Technical Note TN-7 page 5, Geonics Limited, Mississauga, Ontario.

EM Time Constant (Tau) Calculation

The EM Time-Constant (TAU) is a general measure of the speed of decay of the electromagnetic response and indicates the presence of eddy currents in conductive sources as well as reflecting the “conductance quality” of a source. Although TAU can be calculated using either the measured dB/dt decay or the calculated B-field decay, dB/dt is commonly preferred due to better stability (S/N) relating to signal noise. Generally, TAU calculated on base of early time response reflects both near surface overburden and poor conductors whereas, in the late ranges of time, deep and more conductive sources, respectively. For example early time TAU distribution in an area that indicates conductive overburden is shown in Figure 2.

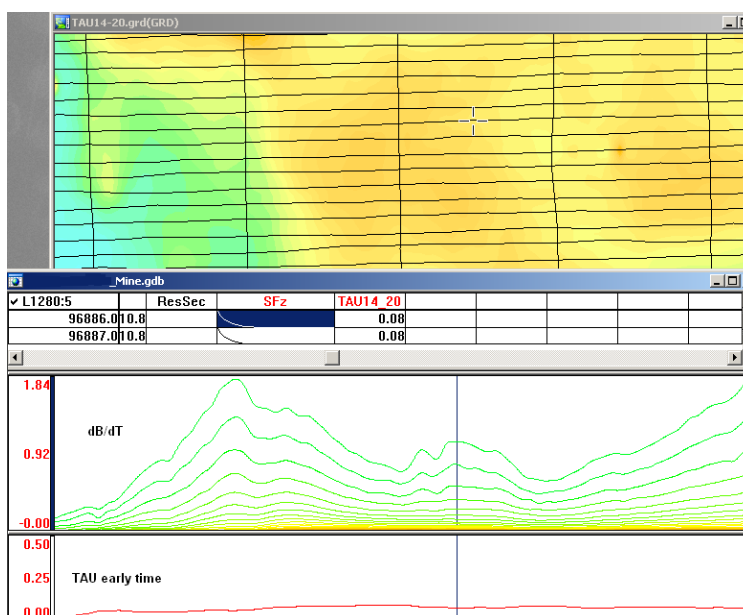


Figure E-2: Map of early time TAU. Area with overburden conductive layer and local sources.

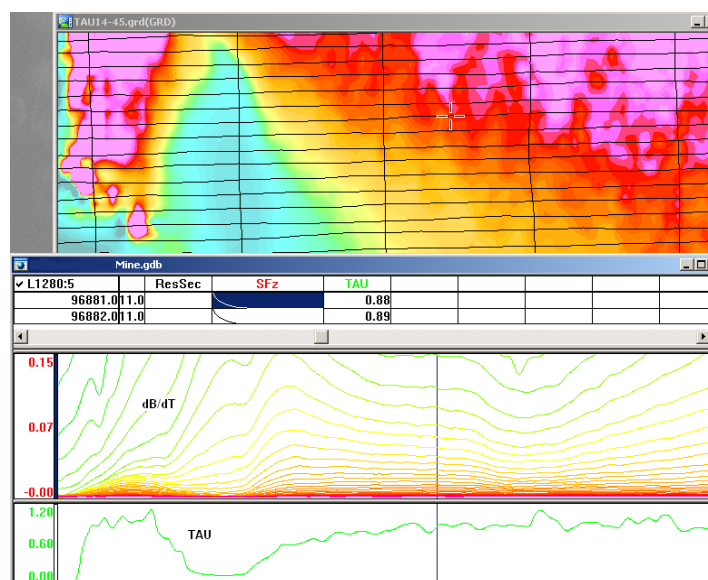


Figure E-3: Map of full time range TAU with EM anomaly due to deep highly conductive target.

There are many advantages of TAU maps:

- TAU depends only on one parameter (conductance) in contrast to response magnitude;
- TAU is integral parameter, which covers time range and all conductive zones and targets are displayed independently of their depth and conductivity on a single map.
- Very good differential resolution in complex conductive places with many sources with different conductivity.
- Signs of the presence of good conductive targets are amplified and emphasized independently of their depth and level of response accordingly.

In the example shown in Figure 4 and 5, three local targets are defined, each of them with a different depth of burial, as indicated on the resistivity depth image (RDI). All are very good conductors but the deeper target (number 2) has a relatively weak dB/dt signal yet also features the strongest total TAU (Figure 4). This example highlights the benefit of TAU analysis in terms of an additional target discrimination tool.

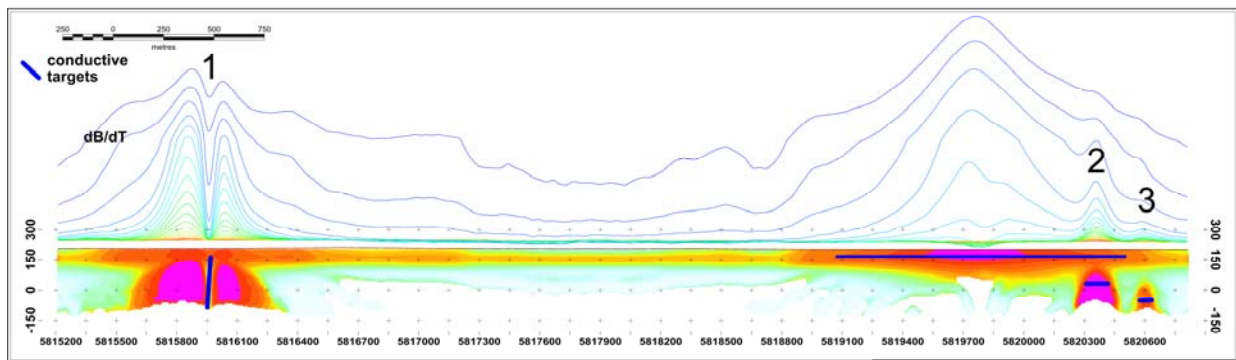


Figure E-4: dB/dt profile and RDI with different depths of targets.

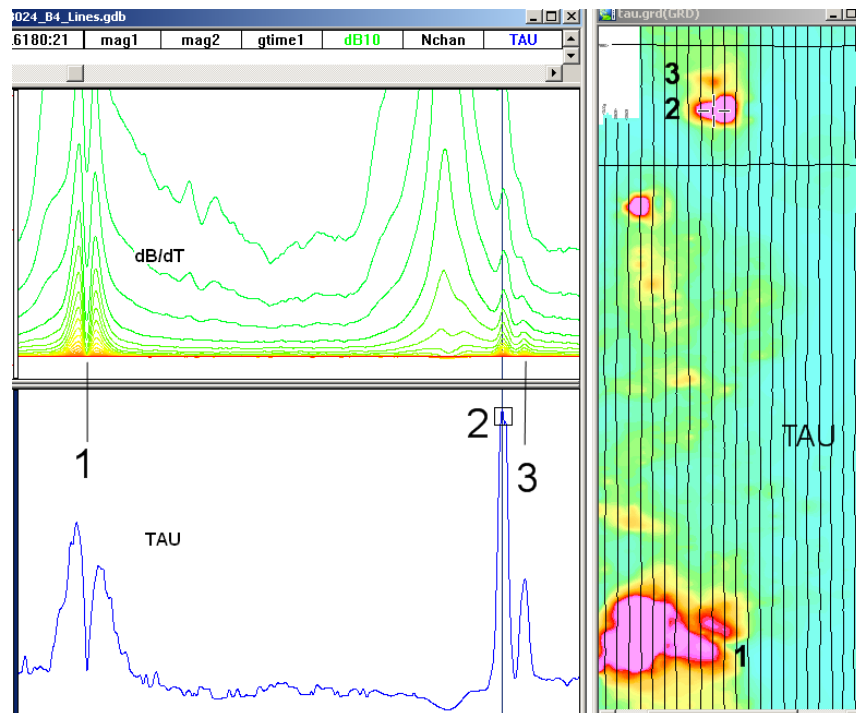


Figure E-5: Map of total TAU and dB/dt profile.

The EM Time Constants for dB/dt and B-field were calculated using the “sliding Tau” in-house program developed at Geotech². The principle of the calculation is based on using of time window (4 time channels) which is sliding along the curve decay and looking for latest time channels which have a response above the level of noise and decay. The EM decays are obtained from all available decay channels, starting at the latest channel. Time constants are taken from a least square fit of a straight-line (log/linear space) over the last 4 gates above a pre-set signal threshold level (Figure F6). Threshold settings are pointed in the “label” property of TAU database channels. The sliding Tau method determines that, as the amplitudes increase, the time-constant is taken at progressively later times in the EM decay. Conversely, as the amplitudes decrease, Tau is taken at progressively earlier times in the decay. If the maximum signal amplitude falls below the threshold, or becomes negative for any of the 4 time gates, then Tau is not calculated and is assigned a value of “dummy” by default.

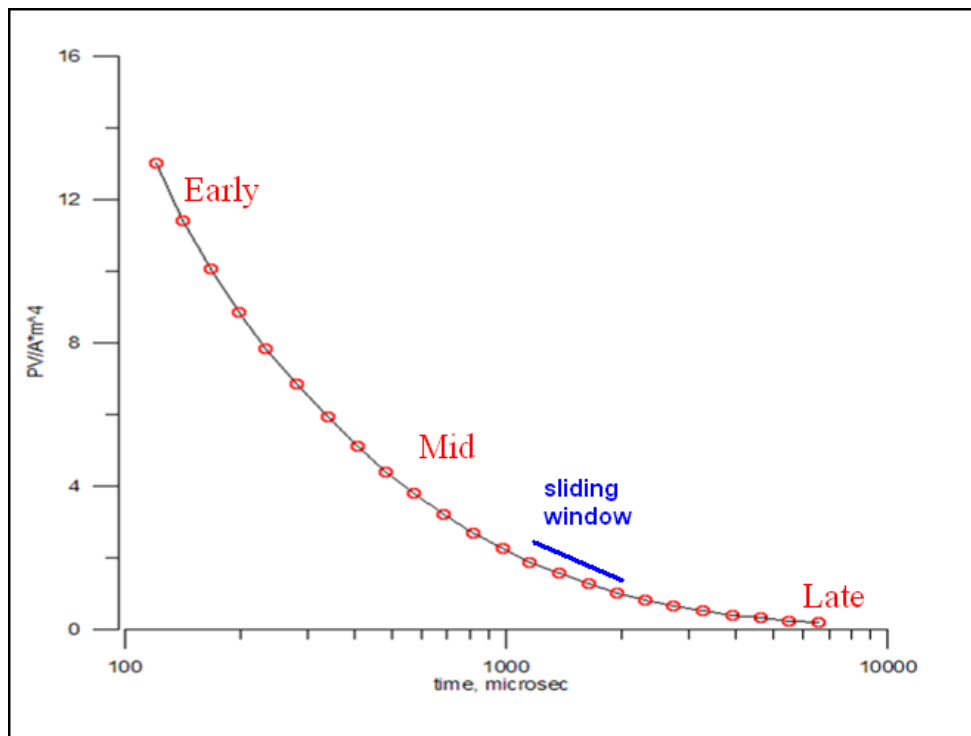


Figure E-6: Typical dB/dt decays of VTEM data

Alexander Prikhodko, PhD, P. Geo
Geotech Ltd.

September 2010

² by A.Prikhodko

APPENDIX F

TEM RESISTIVITY DEPTH IMAGING (RDI)

Resistivity depth imaging (RDI) is a technique used to rapidly convert EM profile decay data into an equivalent resistivity versus depth cross-section, by deconvolving the measured TEM data. The used RDI algorithm of Resistivity-Depth transformation is based on the scheme of the apparent resistivity transform of Maxwell A. Meju (1998)¹ and TEM response from a conductive half-space. The program is developed by Alexander Prikhodko and depth calibrated based on forward plate modeling for VTEM system configuration (Fig. 1-10).

RDI provides reasonable indications of conductor relative depth and vertical extent, as well as accurate 1D layered-earth apparent conductivity/resistivity structure across VTEM flight lines. Approximate depth of investigation of a TEM system, image of secondary field distribution in half-space, effective resistivity, initial geometry and position of conductive targets is the information obtained on the basis of the RDI.

Maxwell forward modeling with RDI sections from the synthetic responses (VTEM system)

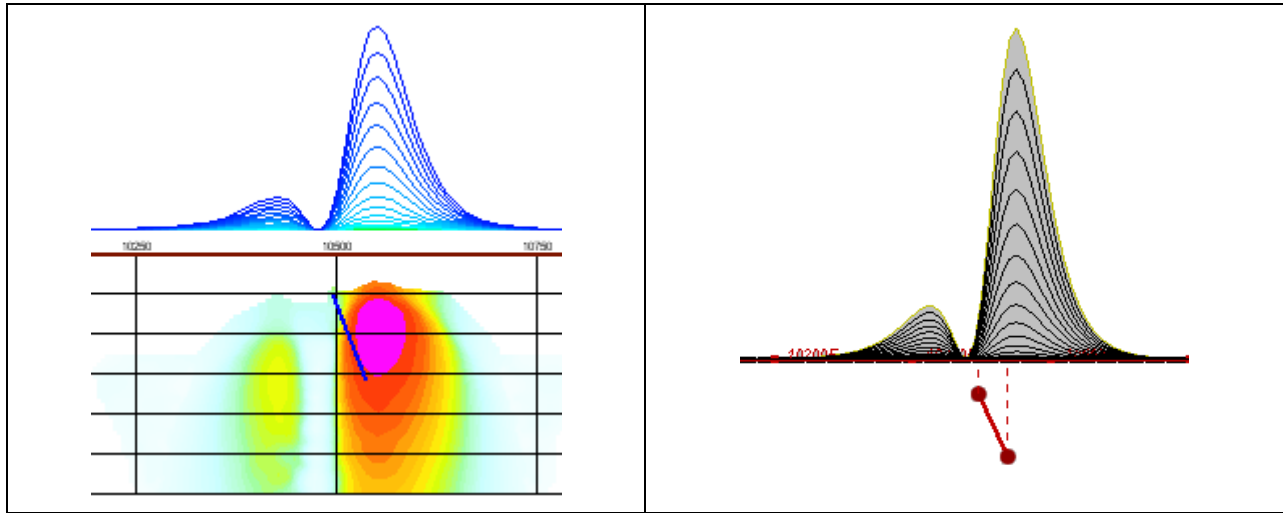


Figure F-1: Maxwell plate model and RDI from the calculated response for conductive “thin” plate (depth 50 m, dip 65 degree, depth extend 100 m).

¹ Maxwell A. Meju, 1998, Short Note: A simple method of transient electromagnetic data analysis, *Geophysics*, **63**, 405–410.

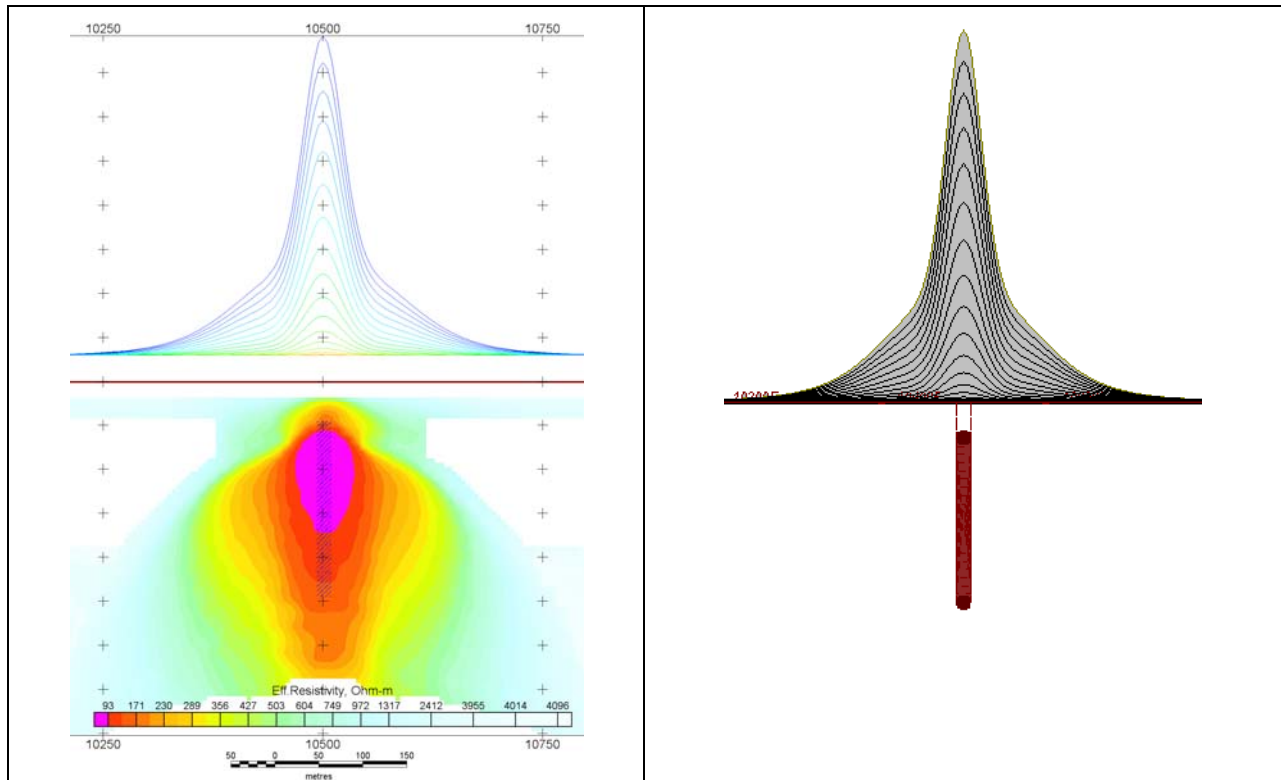


Figure F-2: Maxwell plate model and RDI from the calculated response for “thick” plate 18 m thickness, depth 50 m, depth extend 200 m).

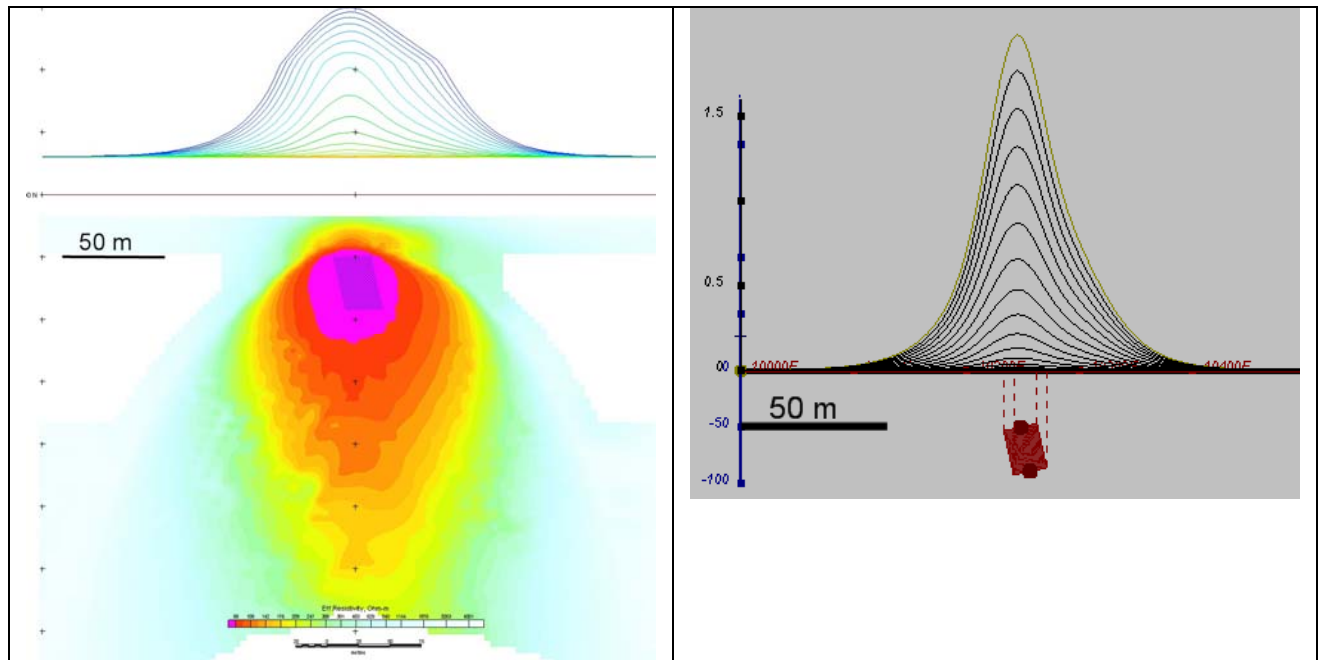


Figure F-3: Maxwell plate model and RDI from the calculated response for bulk (“thick”) 100 m length, 40 m depth extend, 30 m thickness

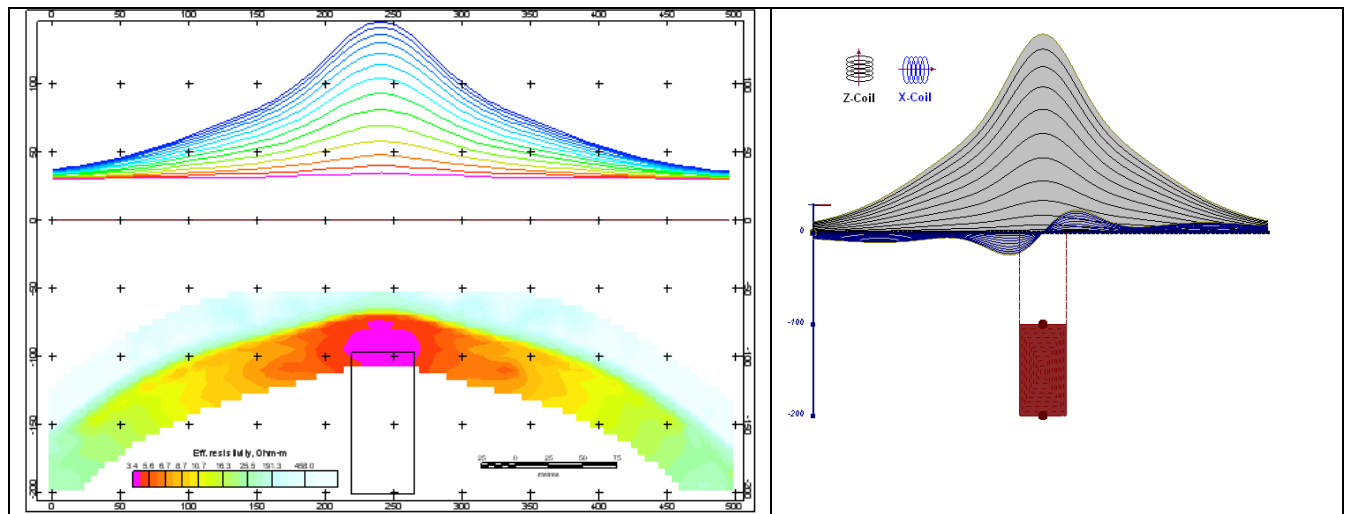


Figure F-4: Maxwell plate model and RDI from the calculated response for “thick” vertical target (depth 100 m, depth extend 100 m). 19-44 chan.

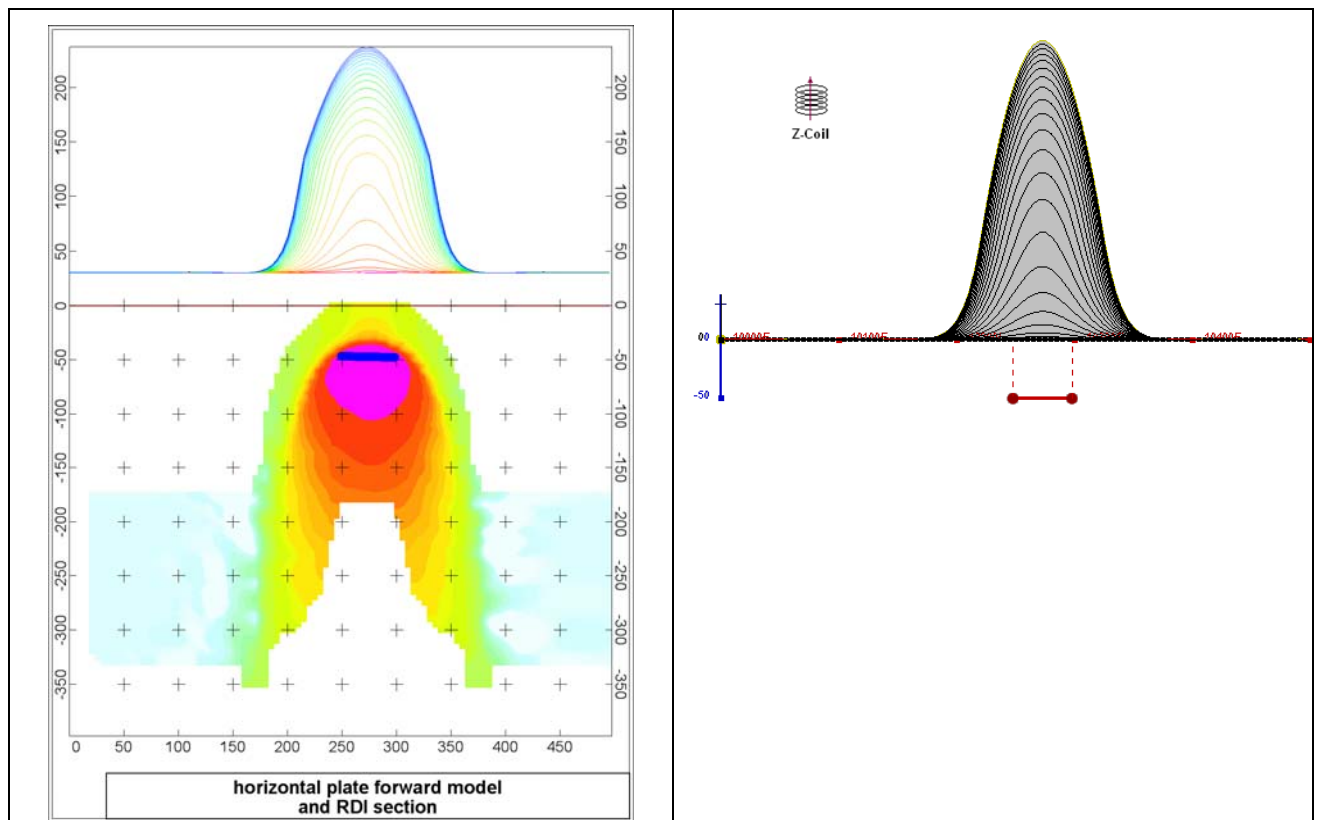


Figure F-5: Maxwell plate model and RDI from the calculated response for horizontal thin plate (depth 50 m, dim 50x100 m). 15-44 chan.

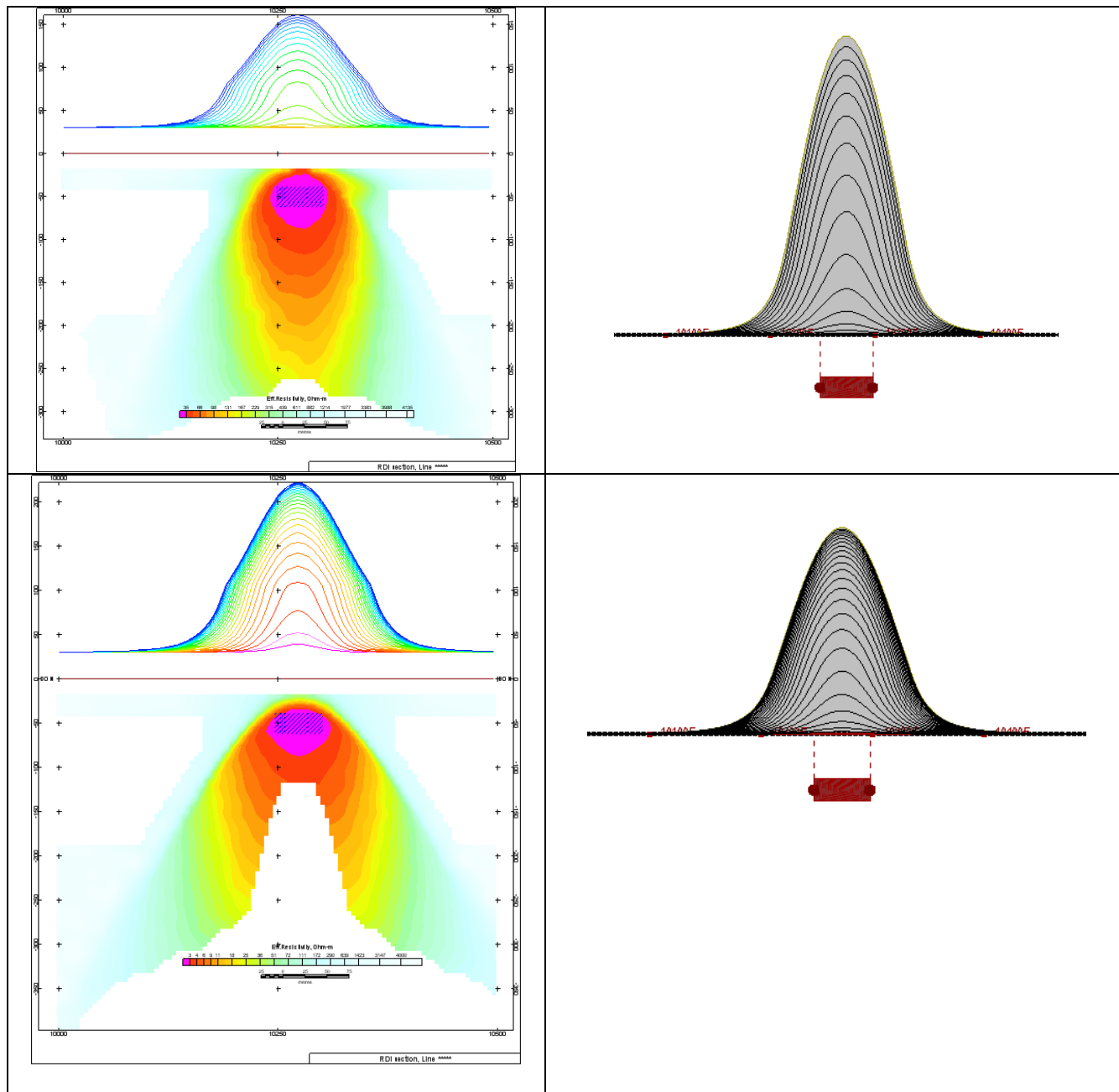


Figure F-6: Maxwell plate model and RDI from the calculated response for horizontal thick (20m) plate – less conductive (on the top), more conductive (below)

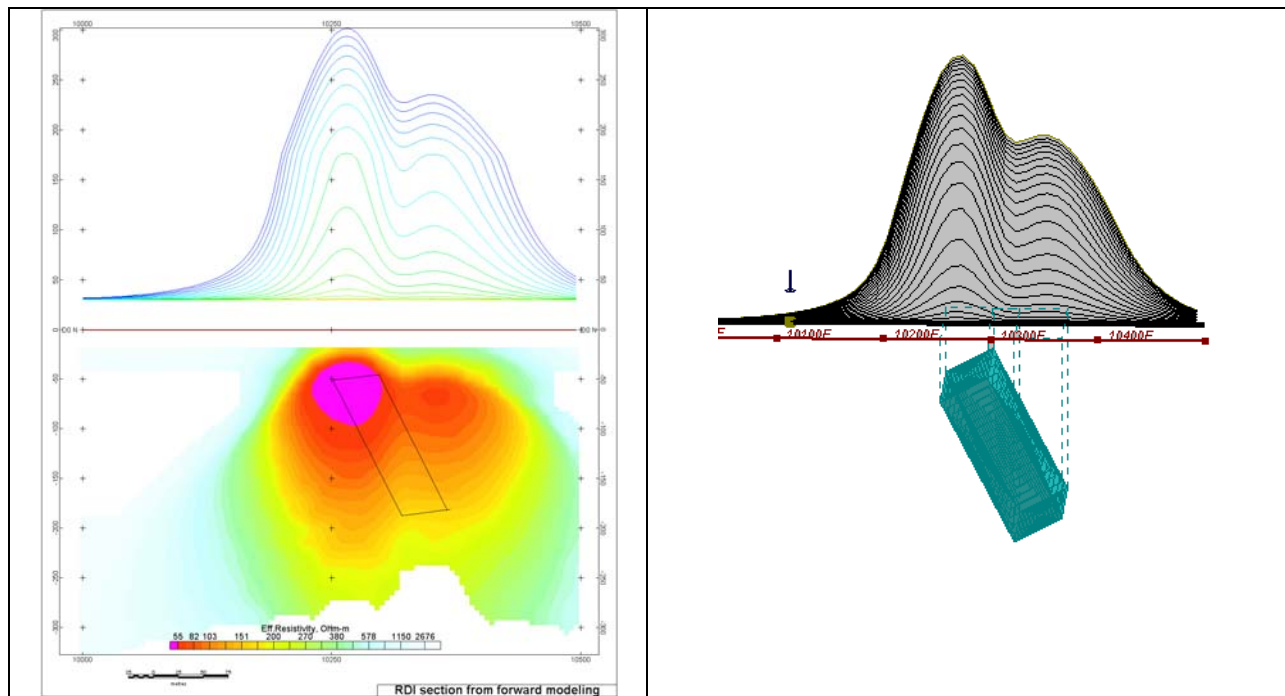


Figure F-7: Maxwell plate model and RDI from the calculated response for inclined thick (50m) plate. Depth extends 150 m, depth to the target 50 m.

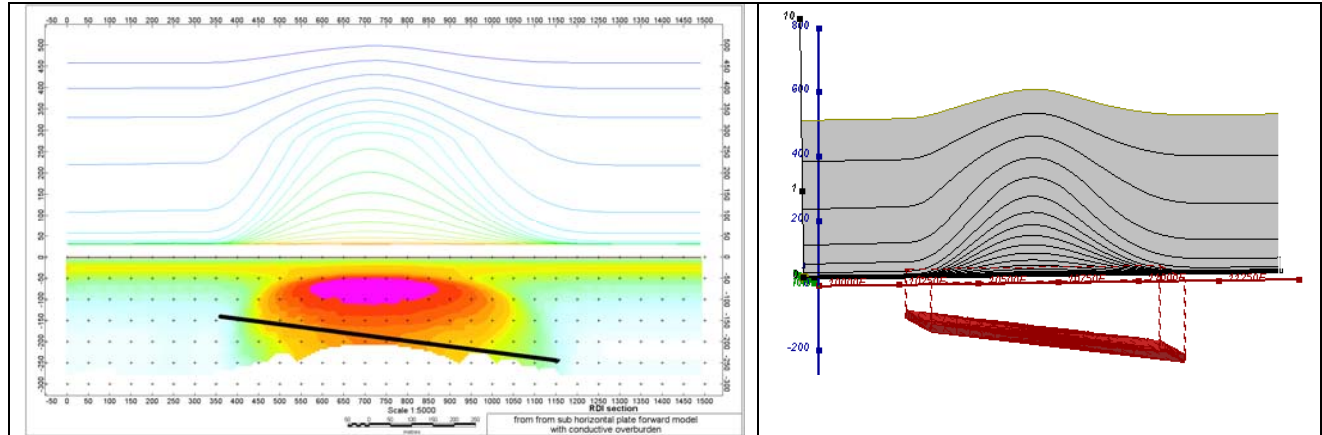


Figure F-8: Maxwell plate model and RDI from the calculated response for the long, wide and deep subhorizontal plate (depth 140 m, dim 25x500x800 m) with conductive overburden.

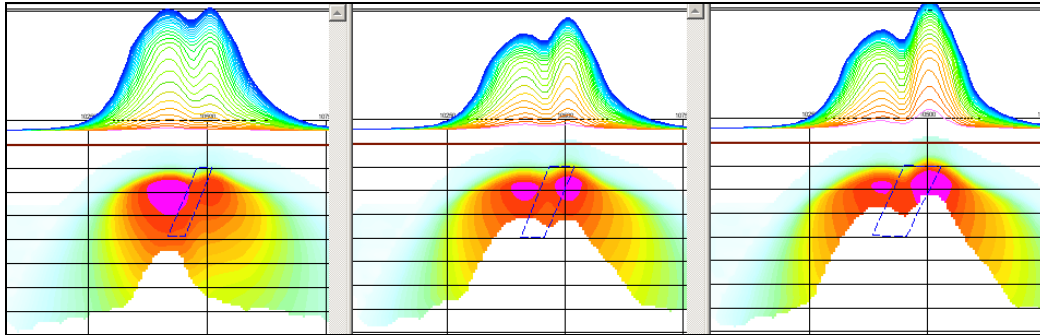


Figure F-9: Maxwell plate models and RDIs from the calculated response for “thick” dipping plates (35, 50, 75 m thickness), depth 50 m, conductivity 2.5 S/m.

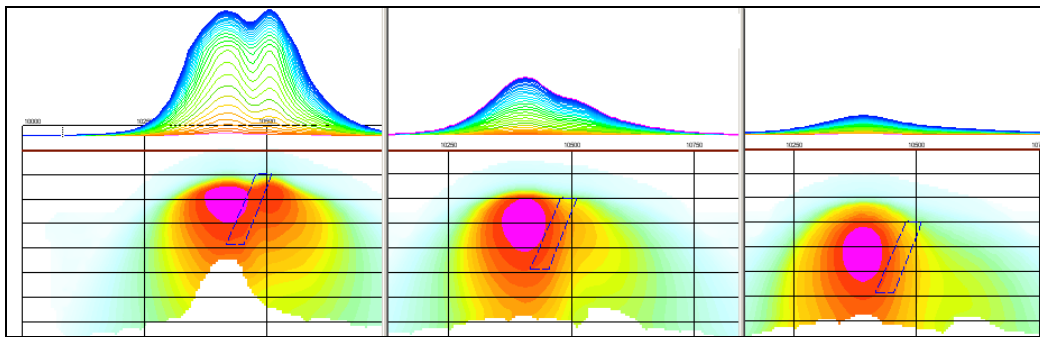


Figure F-10: Maxwell plate models and RDIs from the calculated response for “thick” (35 m thickness) dipping plate on different depth (50, 100, 150 m), conductivity 2.5 S/m.

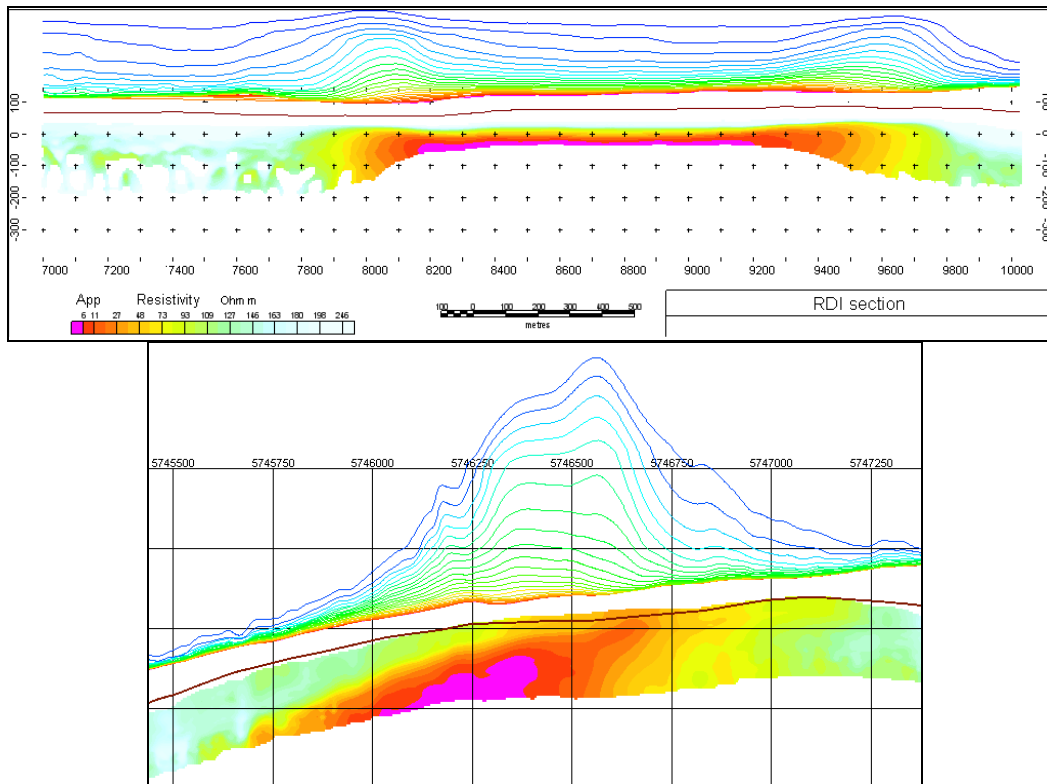
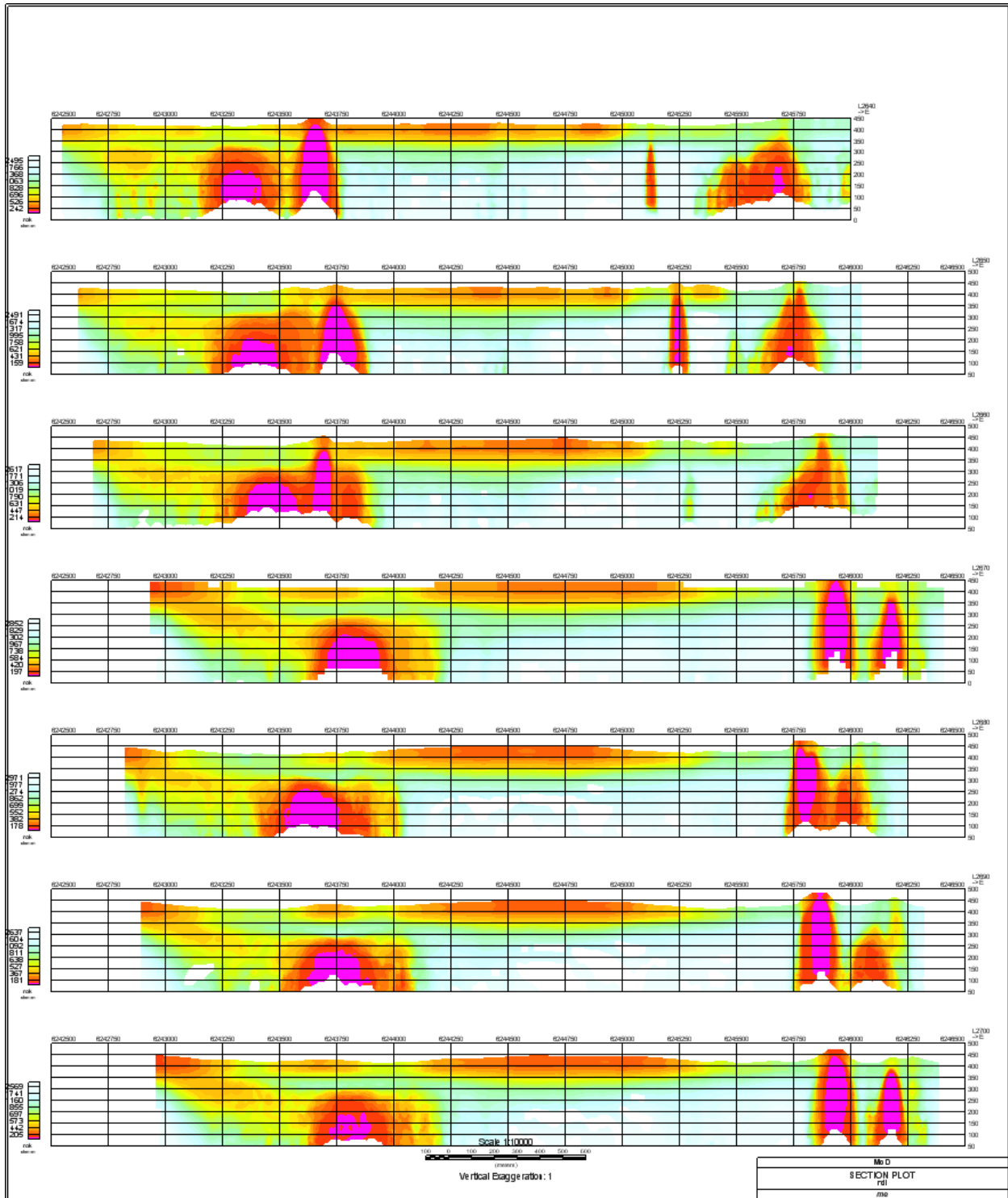


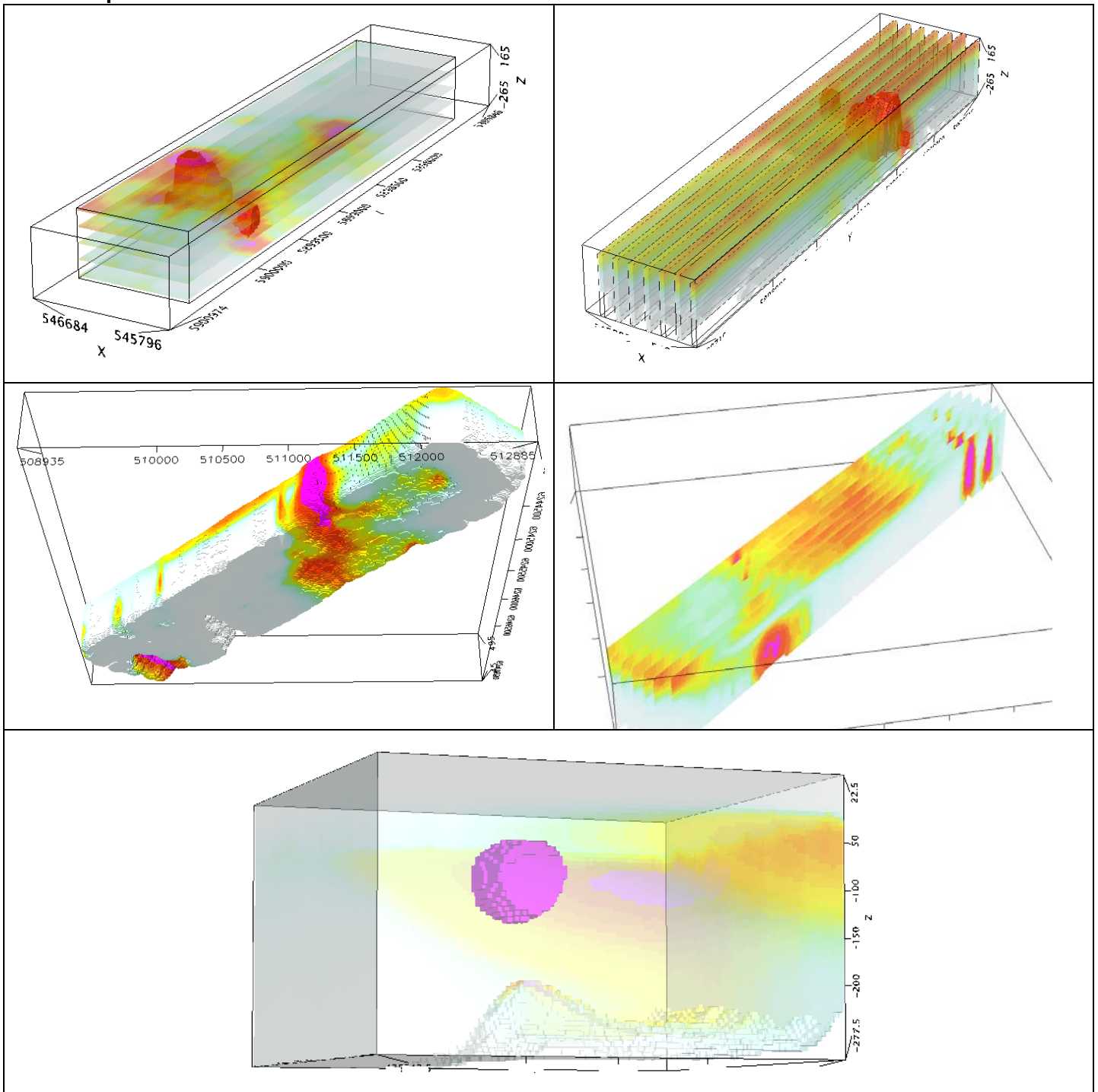
Figure F-11: RDI section for the real horizontal and slightly dipping conductive layers

FORMS OF RDI PRESENTATION

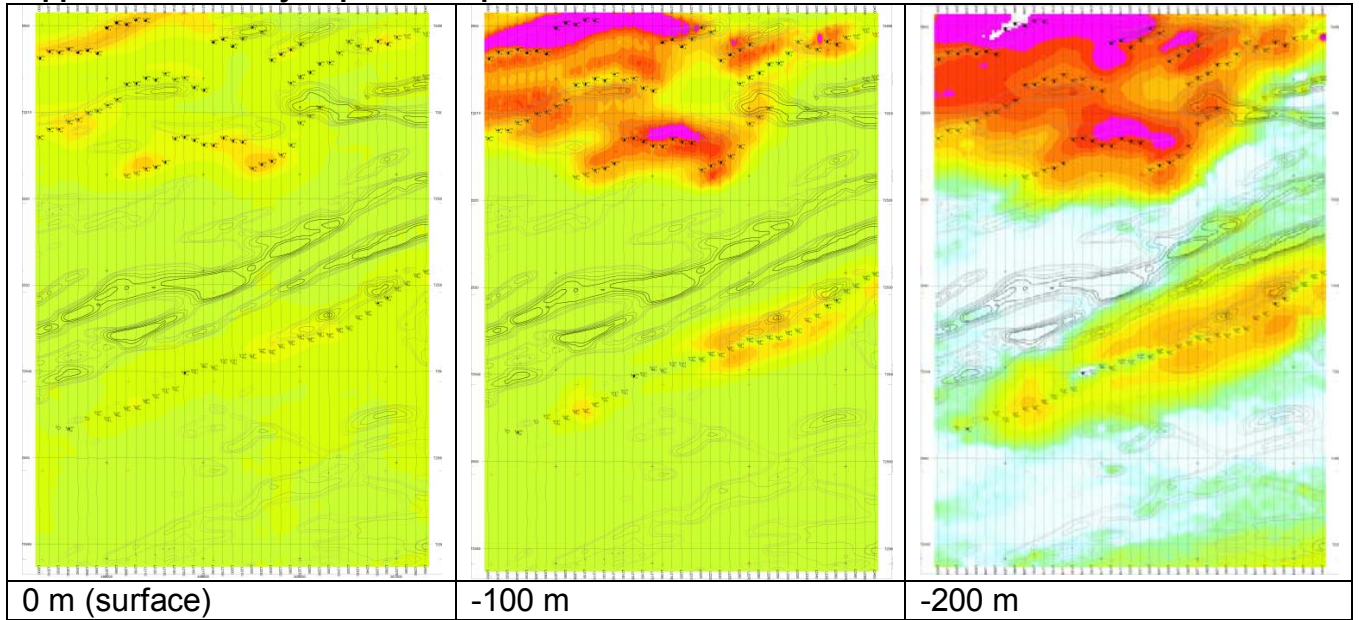
Presentation of series of lines



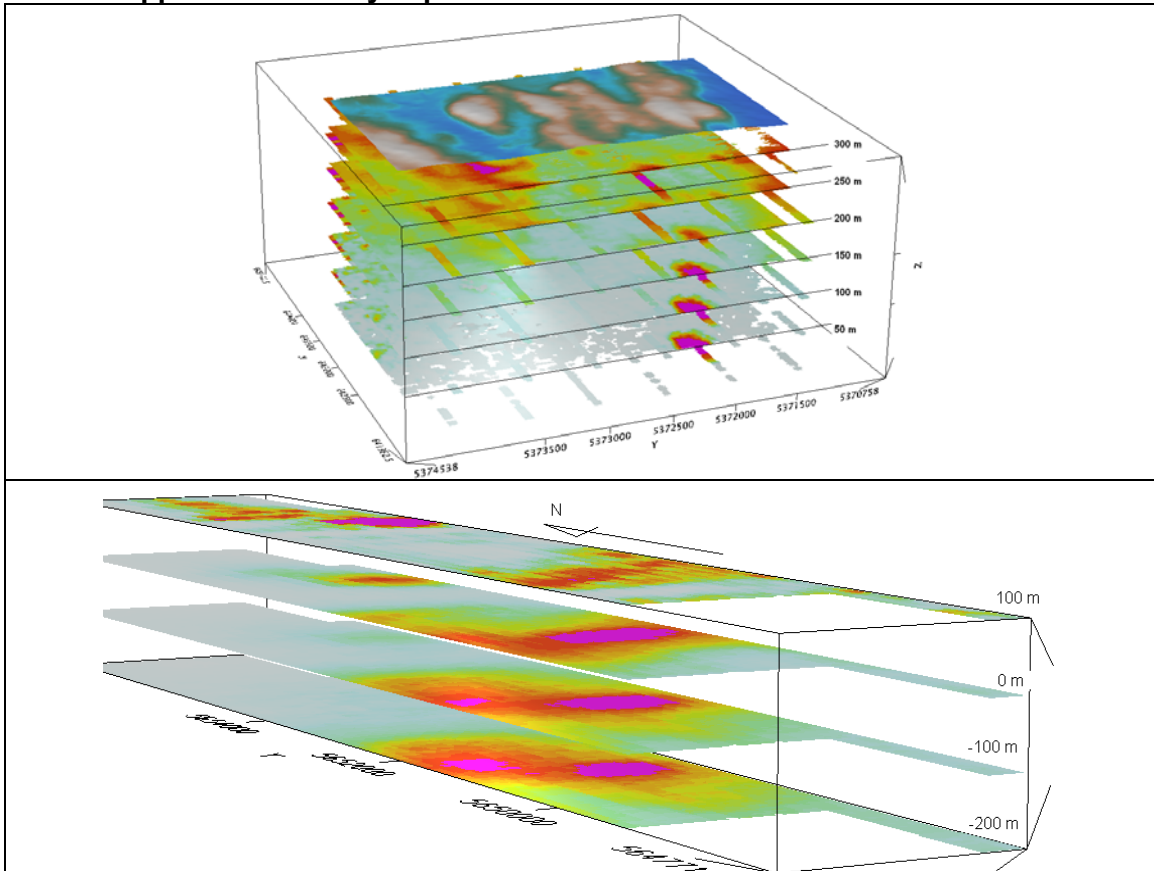
3d presentation of RDIs



Apparent Resistivity Depth Slices plans:

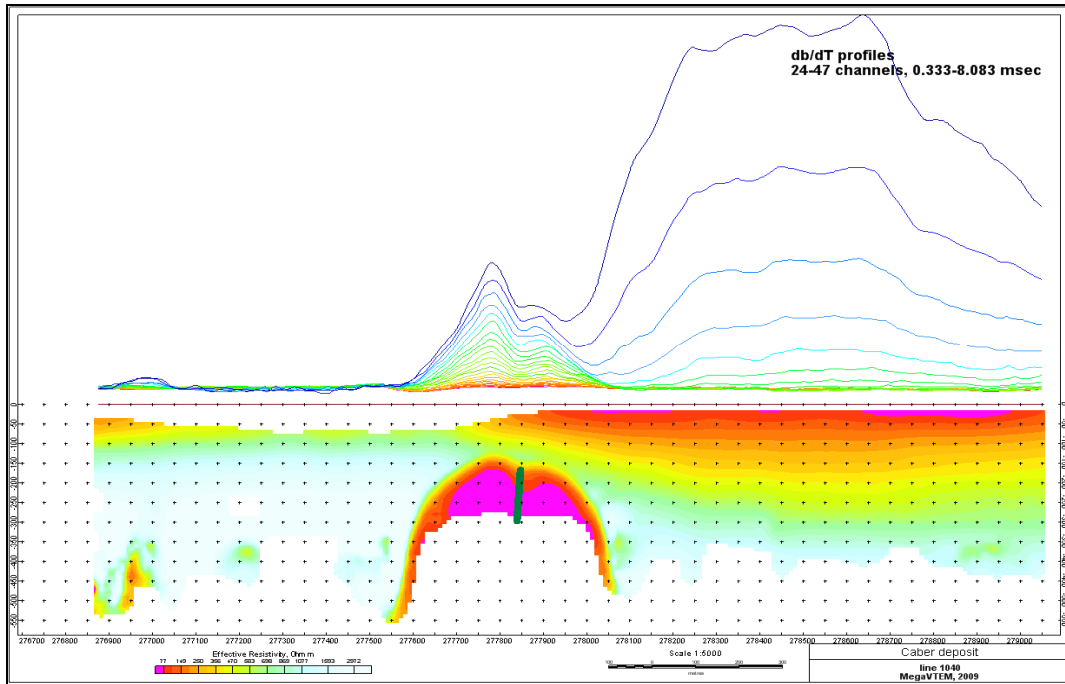


3d views of apparent resistivity depth slices:

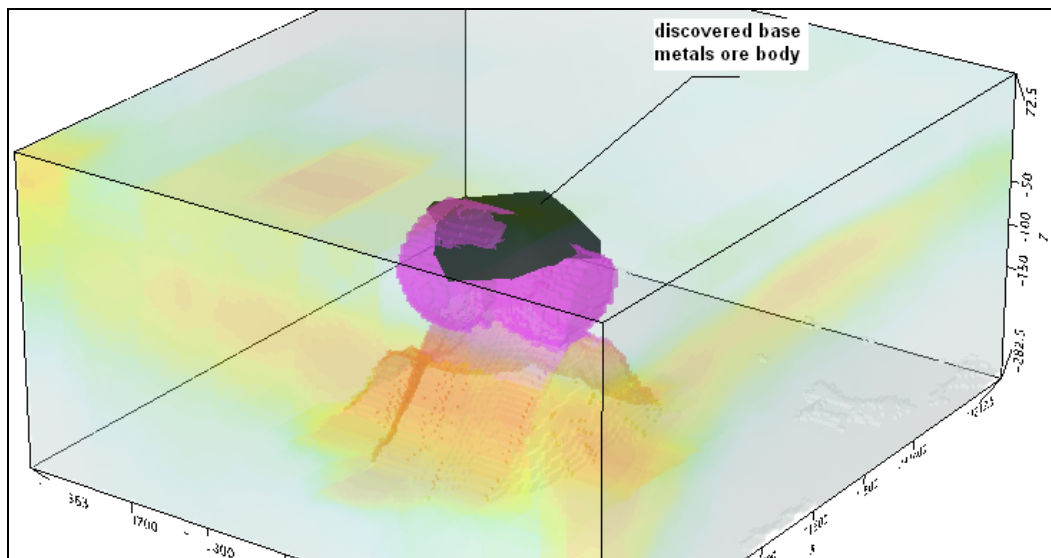


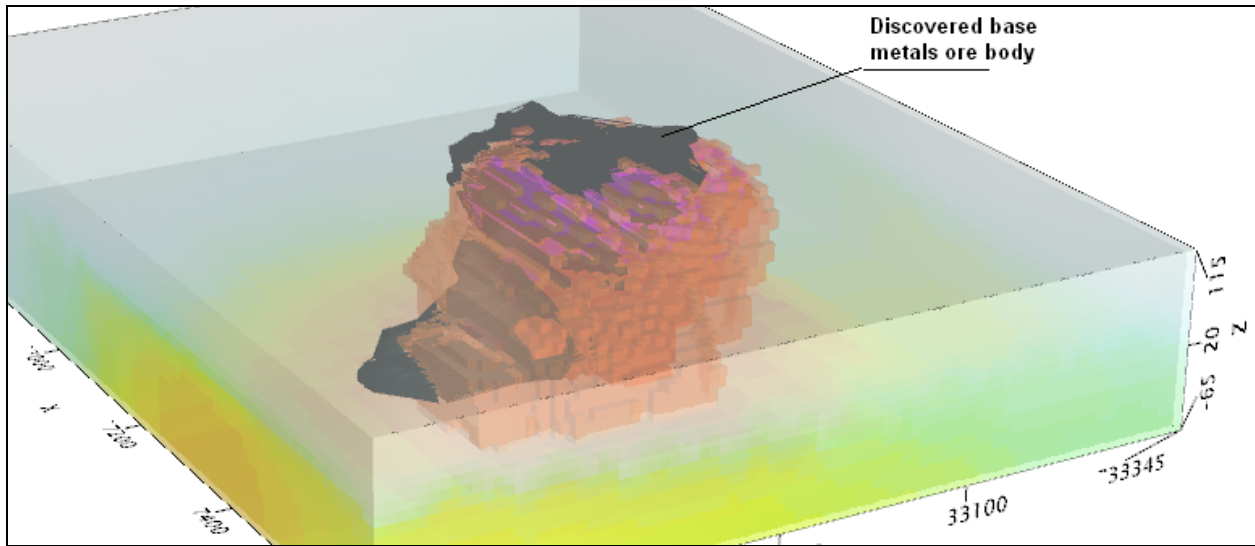
Real base metal targets in comparison with RDIs:

RDI section of the line over Caber deposit (“thin” subvertical plate target and conductive overburden).



3d RDI voxels with base metals ore bodies (Middle East):





Alexander Prikhodko, PhD, P. Geo
Geotech Ltd.
April 2011

APPENDIX G
Resistivity Depth Images (RDI)
Please see RDI Folder on DVD for the PDF's